

Article

# Thermodynamic Overview of Bioconjugation Reactions Pertinent to Lysine and Cysteine Peptide and Protein Residues

Maja Lopandic <sup>†,‡</sup>, Fatima Merza <sup>†,§</sup> and John F. Honek <sup>\*</sup>

Department of Chemistry, University of Waterloo, 200 University Avenue West, Waterloo, ON N2L 3G1, Canada; maja.lopanadic@epfl.ch (M.L.); fatima.mirza96@gmail.com (F.M.)

\* Correspondence: jhonek@uwaterloo.ca; Tel.: +1-1-519-888-4567 (ext. 35817)

<sup>†</sup> These authors contributed equally to this work.

<sup>‡</sup> Current address: Laboratoire des Polymères STI—IMX—LP MXD 112 (Batiment MXD), Institut des Matériaux, Ecole Polytechnique Fédérale de Lausanne (EPFL), Station 12, CH-1015 Lausanne, Switzerland.

<sup>§</sup> Current address: Public Health Ontario, Toronto, ON, M5G 1M1, Canada.

**Abstract:** Bioconjugation reactions are critical to the modification of peptides and proteins, permitting the introduction of biophysical probes onto proteins as well as drugs for use in antibody-targeted medicines. A diverse set of chemical reagents can be employed in these circumstances to covalently label protein side chains, such as the amine moiety in the side chain of lysine and the thiol functionality in cysteine residues, two of the more frequently employed sites for modification. To provide researchers with a thermodynamic survey of the reaction of these residues with frequently employed chemical modification reagents as well as reactive cellular intermediates also known to modify proteins non-enzymatically, a theoretical investigation of the overall thermodynamics of models of these reactions was undertaken at the T1 and G3(MP2) thermochemical recipe levels (gas phase), the M06-2X/6-311+G(2df,2p)/B3LYP/6-31G(d) (gas and water phase), and the M06-2X/cc-PVTZ (-f)++ density functional levels of theory (water phase). Discussions of the relationship between the reagent structure and the overall thermodynamics of amine or thiol modification are presented. Of additional interest are the observations that routine cellular intermediates such as certain thioesters, acyl phosphates, and acetyl-*L*-carnitine can contribute to non-enzymatic protein modifications. These reactions and representative click chemistry reactions were also investigated. The computational survey presented herein (>320 reaction computations were undertaken) should serve as a valuable resource for researchers undertaking protein bioconjugation. A concluding section addresses the ability of computation to provide predictions as to the potential for protein modification by new chemical entities, with a cautionary note on protein modification side reactions that may occur when employing synthetic substrates to measure enzyme kinetic activities.

**Keywords:** chemical modification; bioconjugation; protein modification; density functional theory; computation; thermodynamics; thermochemical; acetyl-*L*-carnitine; thioester; click reactions



**Citation:** Lopandic, M.; Merza, F.; Honek, J.F. Thermodynamic Overview of Bioconjugation Reactions Pertinent to Lysine and Cysteine Peptide and Protein Residues. *Compounds* **2023**, *3*, 464–503. <https://doi.org/10.3390/compounds3030035>

Academic Editor: Juan C. Mejuto

Received: 24 July 2023

Revised: 24 August 2023

Accepted: 25 August 2023

Published: 30 August 2023



**Copyright:** © 2023 by the authors. Licensee MDPI, Basel, Switzerland. This article is an open access article distributed under the terms and conditions of the Creative Commons Attribution (CC BY) license (<https://creativecommons.org/licenses/by/4.0/>).

## 1. Introduction

Chemical modification and attachment of biophysical probes to biomolecules is an important strategy in the biological sciences, as the approach allows for biological imaging and the study of the proximity and dynamics of sections of a protein when employing fluorescence or spin-labeling techniques [1–9]. In addition, the bioconjugation of molecules to a protein's surface can allow for protein and virus immobilization onto surfaces [10–12], the attachment of drug molecules to antibodies for directed chemotherapy [13–15], the introduction of polyethylene glycol (PEG) polymers to control immunogenicity and pharmacodynamics of therapeutic proteins [16,17], and the crosslinking of biomolecules using homobifunctional or heterobifunctional crosslinking agents for the fabrication of new biomaterials or the preparation of proteolysis targeting chimera (PROTACS) for developing new modalities for enzyme inhibition [18,19]. Underpinning these initiatives is

the chemistry that allows for the attachment process itself. Although unnatural amino acid incorporation into peptides and proteins can be employed to provide the necessary reactive moieties to allow for the required chemistry [20–24], the use of chemically reactive reagents in labeling nucleophilic protein side chains such as lysine and cysteine remains the predominant approach undertaken by researchers [8]. In fact, a vast array of commercially available chemical modification reagents, containing such reactive moieties as N-hydroxysuccinimide (NHS) esters and maleimide groups, make routine biomolecule modification readily attainable for even researchers who are less experienced with the chemical intricacies of the bioconjugation process [4]. Companies such as Quanta BioDesign, Ltd., BroadPharm, and Click Chemistry Tools, among others, provide valuable sources of these reagents for scientists.

Underlying the chemistry of these reactions are the kinetic and thermodynamic properties of the reactions themselves and how this information can inform researchers as to the potential success or failure of a particular bioconjugation approach and, more fundamentally, the relationship of chemical structure to the overall reaction outcome. Bioconjugation reactions on protein residues are complex processes with differential reaction kinetics for a particular reagent in multiple but different environments containing the same residue (such as multiple lysine residues on the surface of a protein) along with the differential reaction rates of that same reagent with different residue types (such as lysine versus cysteine residues for a reagent able to react with both). In essence, bioconjugation reactions are simple in theory but complex in experimental reality, generally leading to an ensemble of modified protein products. The thermodynamics of the overall labeling reaction are also of importance, allowing for metrics on the favorability of a specific reagent's chemical reaction with an amino acid functional group. In the case of bioconjugation reactions, experimentalists employ sufficient time for the reaction to occur and follow the extent of protein modification by mass spectrometry, for example. Hence, although the rate may be slower, which would depend on the energy of the transition state, the incubation time of the protein with the reagent is adjusted to optimize the labeled protein. Experimentally, incubation times can vary from minutes to hours, depending on the modification reagent. The time of incubation, pH, excess of the modification reagent, and temperature are all controlled to optimize the yield of a labeled protein. In general, the optimized modification conditions for any particular protein are empirically determined for each reagent that is used. In our own research on the chemical modification of bacteriophage for bionanotechnological applications [25,26], it was of interest to have a readily available source of information on the overall thermodynamics of the most frequently employed bioconjugation reactions employed in biological chemistry. Sadly, we could not find such a single compendium of this information, but rather fragmented studies with theoretical or experimental studies focused upon a single reaction type and employing different levels of theoretical computation, resulting in difficulty in comparing the thermodynamic range of chemical modification reactions available.

This report therefore has focused on generating these thermodynamic properties by density functional theory (DFT) for a range of commonly used bioconjugation reactions for lysine (modeled as methylamine) and cysteine (modeled as methanethiol) residues (Figure 1), comparing these to several representative “click” reactions [27–29], and addressing the energetics of several previous observations that certain cellular intermediates (thioesters, acyl phosphates, and acetyl-*L*-carnitine) are capable of non-enzymatically modifying proteins in vivo [30–35]. A concluding section addresses the ability of computation to provide predictions as to the potential for protein modification by new chemical entities, with a cautionary note on protein modification side reactions when employing synthetic substrates to measure enzyme kinetic activities.

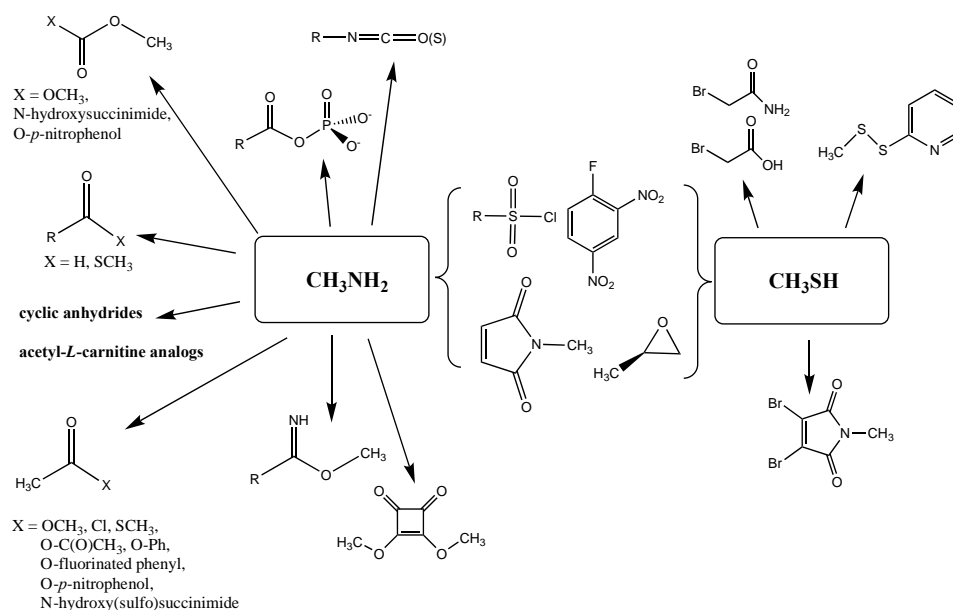


**Figure 1.** Overview of the reactions of lysine (modeled as methylamine) and cysteine (modeled as methanethiol) residues with a range of bioconjugation reagents and cellular metabolites whose thermodynamic reaction parameters are computed in the manuscript.

## 2. Materials and Methods

Spartan'20 (Wavefunction, Inc.; Irvine, CA, USA) [36] was employed for T1 and G3(MP2) thermochemical recipe calculations and the density functionals, B3LYP [37,38] and M06-2X [39], were employed in M06-2X/6-311+G(2df,2p)//B3LYP/6-31G(d) density functional theory (DFT) calculations to compute overall reaction thermodynamic properties for a diverse set of chemical modification reactions [40]. Water, methylamine, and methanethiol were used as reactants; methylamine was used to model the primary amine of the lysine side chain and methanethiol to model the cysteine side chain. The protonated, positively charged amine is non-nucleophilic and experimentally the bioconjugation of lysine residues is performed at a pH where a percentage of the lysine side chains are deprotonated (neutral) and reactive. This occurs prior to the actual chemical reaction between the deprotonated amine and the reagent and is taken care of by the solution pH, using a buffer, for example. Therefore, the free energy penalty to deprotonate is paid for macroscopically by the experimental conditions. We employ this neutral amine in the form of methylamine as the model for the lysine side chain as well as the N-terminal nitrogen of a protein subunit. The neutral form of the thiol in cysteine is used in this study by employing methanethiol as the model for the side chain of cysteine. An experimental choice of a solution pH that maintains the protonated unreactive form of lysine residues but allows for the reaction of the neutral thiol is frequently employed, and hence the neutral thiol group is employed in the current computational study. The chemical structures of reactants and products were drawn with the molecule drawing palette in Spartan'20. For T1 [41] and G3(MP2) [42] calculations, the Equilibrium Conformer setting was used to provide the global minimum conformation as the starting conformation for these gas phase thermochemical calculations. This involved the selection of the lowest energy conformer through a molecular mechanics conformational search for the lowest energy conformer using the Merck molecular force field (MMFF) [43,44], followed by energy ranking at the HF/6-31G(d) geometry optimization in the T1 model.

In vacuum, the T1 and G3(MP2) composite methods, also known as thermochemical recipes, are computational methods that provide high accuracy for gas phase thermodynamic quantities and are composed of several calculation stages. A full description of the G3(MP2) and the T1 methods has been reported [41,42]. In brief, the G3(MP2) recipe requires an equilibrium geometry calculation at the HF/6-31G(d) level, followed by a second

at the MP2/6-31G(d) level. This is followed by an HF/6-31G(d) frequency calculation, an MP2/6-311++G(2df,2p) energy calculation, and a QCISD(T)/6-31G(d) energy calculation. The T1 method was specifically developed to provide a more efficient procedure than the more complex G3(MP2) method (providing a reduction in computational cost of 2–3 orders of magnitude over the G3(MP2) method) for calculating heats of formation of uncharged, closed-shell molecules comprising H, C, N, O, F, S, Cl, and Br in the gas phase and able to reproduce G3(MP2) computed properties with mean absolute and root mean square errors of 1.8 and 2.5 kJ/mol, respectively [41]. T1 introduces an empirical correction based on Hartree–Fock and RI-MP2 energies and Mulliken bond orders, among other modifications. Readers may also find the Computational Chemistry Comparison and Benchmark DataBase (<https://cccbdb.nist.gov> (accessed on 24 August 2023)) a useful resource for pre-calculated gas phase energies for some molecules [45].

The M06-2X/6-311+G(2df,2p)//B3LYP/6-31G(d) calculations were computed for both vacuum as well as implicit aqueous conditions starting from the equilibrium geometry obtained by a B3LYP/6-31G(d) geometry optimization, a robust model for producing optimized geometries, and have recently been employed in computing the reaction thermodynamics for thiol addition to various Michael acceptor molecules [40,46,47]. This was followed by a single-point M06-2X/6-311+G(2df,2p) calculation [39,40]. Vibrational frequencies and zero-point energies were calculated at the B3LYP/6-31G(d) level and were evaluated analytically and uniformly scaled by a factor of 0.960 [48]. No negative frequencies were detected for any geometry-optimized structures employed in this investigation. The conductor-like polarizable continuum model (C-PCM) solvent model for water with a dielectric constant of 78 was used for aqueous conditions [49,50]. This cosolvent model is dependent upon the shape and charge distribution of the solute and the dielectric constant (value of 78) for water.

Jaguar (Schrödinger, LLC, New York, NY, USA) [51] was employed for both gas phase and implicit water phase calculations of other reactions at the M06-2X/cc-PVTZ(-f)++ density functional theory level. This method employs the pseudospectral method, which is reported to enhance calculations on larger molecular systems [51,52]. Chemical structures were sketched in the Maestro drawing palette (Schrödinger Release 2023-2: Maestro, Schrödinger, LLC, New York, NY, USA, 2023). The lowest energy conformations in water were then calculated employing the QM Conformer and Tautomer Predictor panel, employing solely the conformer submodule as alternate tautomers were not required for the compounds investigated in this study. This workflow generates a range of lower-energy conformers using the OPLS4 molecular mechanics force field implemented in the MacroModel program (Schrödinger Release 2023-2: MacroModel, Schrödinger, LLC, New York, NY, USA, 2023) [53–55]. The resulting molecular structures are then filtered by their semiempirical PM3 heat of formation, which removes high-energy conformations [56,57]. The structures surviving these initial screens were then geometry optimized using density functional theory (DFT) at the B3LYP-D3/LACVP\*\* level of theory. The structures are then ranked using single-point energies at the M06-2X/cc-pVTZ(-f) calculated at the optimal geometries from the B3LYP-D3/LACVP\*\* step. The five lowest energy conformers are kept, and the lowest energy conformer is employed in the reaction calculation protocol as implemented in Jaguar, which employed the M06-2X/cc-PVTZ(-f)++ density functional theory level and used the conductor-like screening model (COSMO), a continuum solvation model, with Bondi atomic radii [50,58,59]. Other settings were grid density = fine and an SCF accuracy level = accurate. No negative frequencies were obtained in these computations. The thermodynamic parameters  $\Delta E$  (gas),  $\Delta E$  (water),  $\Delta G$  (water), and  $\Delta H$  (water) were requested in the reaction protocol. A Boltzmann distribution of conformers is not employed in the current study, and only the lowest energy conformer for the various reactants and products is employed throughout the current investigation.

### 3. Results and Discussion

As numerous lysine modification reagents are based on acylation chemistry [4,8], we benchmarked the computational survey of chemical modification reagents against the overall reaction thermodynamics computed for ester hydrolysis and aminolysis using methyl acetate as the ester and either H<sub>2</sub>O or methylamine (lysine side chain model) as the nucleophiles. For reactions modeling the reaction of the cysteine side chain with a bioconjugation reagent, methanethiol was employed. The overall reaction thermodynamic parameters,  $\Delta E$ , Gibbs free energies ( $\Delta G$ ), and enthalpies ( $\Delta H$ ) were calculated at the M06-2X/6-311+G(2df,2p)//B3LYP/6-31G(d) level for the survey of a diverse set of modification reagents and at the M06-2X/cc-PVTZ(-f)++ level for the more focused investigation of several “Click” chemistry reactions [29], and several naturally occurring reactive cellular intermediates (thioesters, anhydrides, acyl-*L*-carnitine) which have been shown to non-enzymatically modify proteins [30,33,35,60,61]. The choice of the basis sets and the functionals employed are frequently employed and have been shown to provide high-quality geometries and energies [37–40,46]. Gas phase as well as polarizable continuum model (PCM)-based intrinsic water phase geometries and energies were computed using the C-PCM and the related COSMO models [49,58]. These models have been reviewed and have been shown to perform well for aqueous phase calculations [50]. In addition, the high-quality thermochemical recipes represented by T1 [41] and G3(MP2) [42] were also employed to provide information on gas phase energetics for the indicated reactions. T1 provides gas phase energies at a lower computational cost than the more elaborate G3(MP2), but within a very good range of the G3(MP2) values, as can be seen from Tables 1 and S1–S9. To note, the computations in this preliminary survey do not take into account the ionic strength or pH of the solution, nor the presence of ions such as Mg<sup>2+</sup> for example. It also does not model the transition states expected at various pHs, which would provide information on the rates of the reactions. A broad survey such as this would be an excellent addition to be undertaken in the future. However, where currently available in the literature, we do provide information on such transition states studied under the conditions investigated by researchers. It is important to note that the absolute values of the total energies for the various reactions computed in this paper are approximate and dependent upon the choice of DFT functional and base set; however, the focus herein is to determine the *relative* reaction thermodynamic values across the different chemistries employed in frequently utilized bioconjugation reactions.

#### 3.1. Lysine Bioconjugation Reactions

##### 3.1.1. Alkyl Esters and Thioesters, Anhydrides, and Acyl Chlorides

We begin with evaluating the T1 and G3(MP2) reaction energetics for a standard ester such as methyl acetate (1) and compare this to extremely reactive chemical reagents such as acetic anhydride (2), acetyl chloride (3), and a simple thioester, methyl thioacetate (4). Anhydrides and acyl chlorides have a long history of use in protein/peptide modification [3,4,62,63]. Cyclic anhydrides have also been suggested as useful bioconjugation reagents and will be discussed in a later section (Section 3.4.1) [64]. Computed T1 and G3(MP2) gas phase reaction energies, shown in Table 1, are more negative for amine reactions than water as the attacking nucleophile for all of the reactions shown (ester, anhydride, acyl chloride, and thioester), with acetic anhydride and acetyl chloride having the greatest reaction energies. Thioester reactions are intermediate in magnitude. We will further elaborate on the reactivity of the anhydrides and thioesters of several important cellular intermediates later in this article, but we present these reference reactions in Table 1. Table 2 provides the M06-2X/6-311+G(2df,2p)//B3LYP/6-31G(d) reaction energies in the gas phase and in the C-PCM intrinsic aqueous phase for these reactions. The trend is identical in that methylamine reactions are more thermodynamically favorable than reactions with H<sub>2</sub>O and that anhydride and acyl chloride reactions are the most favorable of the four different carbonyl compounds.

**Table 1.** T1 and G3(MP2) energies for reaction of water and methylamine with example esters, anhydrides, acetyl chloride, and thioesters.

Reaction	T1 $\Delta E$ (kJ/mol)	G3(MP2) $\Delta E$ (kJ/mol)
$\text{H}_3\text{C}-\text{C}(=\text{O})-\text{O}-\text{CH}_3 + \text{H}-\text{O}-\text{H} \rightleftharpoons \text{H}_3\text{C}-\text{C}(=\text{O})-\text{OH} + \text{H}_3\text{C}-\text{OH}$ <p>1</p>	19.45	22.65
$\text{H}_3\text{C}-\text{C}(=\text{O})-\text{O}-\text{CH}_3 + \text{H}_3\text{C}-\text{NH}_2 \rightleftharpoons \text{H}_3\text{C}-\text{C}(=\text{O})-\text{N}(\text{H})-\text{CH}_3 + \text{H}_3\text{C}-\text{OH}$ <p>1</p>	-2.28	-2.87
$\text{H}_3\text{C}-\text{C}(=\text{O})-\text{O}-\text{C}(=\text{O})-\text{CH}_3 + \text{H}-\text{O}-\text{H} \rightleftharpoons \text{H}_3\text{C}-\text{C}(=\text{O})-\text{OH} + \text{H}_3\text{C}-\text{C}(=\text{O})-\text{OH}$ <p>2</p>	-48.45	-45.34
$\text{H}_3\text{C}-\text{C}(=\text{O})-\text{O}-\text{C}(=\text{O})-\text{CH}_3 + \text{H}_3\text{C}-\text{NH}_2 \rightleftharpoons \text{H}_3\text{C}-\text{C}(=\text{O})-\text{N}(\text{H})-\text{CH}_3 + \text{H}_3\text{C}-\text{C}(=\text{O})-\text{OH}$ <p>2</p>	-70.18	-70.86
$\text{H}_3\text{C}-\text{C}(=\text{O})-\text{Cl} + \text{H}-\text{O}-\text{H} \rightleftharpoons \text{H}_3\text{C}-\text{C}(=\text{O})-\text{OH} + \text{H}-\text{Cl}$ <p>3</p>	-43.00	-38.25
$\text{H}_3\text{C}-\text{C}(=\text{O})-\text{Cl} + \text{H}_3\text{C}-\text{NH}_2 \rightleftharpoons \text{H}_3\text{C}-\text{C}(=\text{O})-\text{N}(\text{H})-\text{CH}_3 + \text{H}-\text{Cl}$ <p>3</p>	-64.73	-63.77
$\text{H}_3\text{C}-\text{C}(=\text{O})-\text{S}-\text{CH}_3 + \text{H}-\text{O}-\text{H} \rightleftharpoons \text{H}_3\text{C}-\text{C}(=\text{O})-\text{OH} + \text{HS}-\text{CH}_3$ <p>4</p>	-10.29	-5.82
$\text{H}_3\text{C}-\text{C}(=\text{O})-\text{S}-\text{CH}_3 + \text{H}_3\text{C}-\text{NH}_2 \rightleftharpoons \text{H}_3\text{C}-\text{C}(=\text{O})-\text{N}(\text{H})-\text{CH}_3 + \text{HS}-\text{CH}_3$ <p>4</p>	-32.02	-31.34

The reaction mechanisms, including acid- and base-catalyzed hydrolysis and aminolysis of esters, have been investigated by a number of research groups and have provided atomistic-level detail of the steps and transition states of these reactions [65–78] (and references therein). For example, the methanolysis and hydrolysis of glycerol triacetate have been studied employing B3LYP/6-31++G(d,p)-level DFT methods with a C-PCM continuum solvation model, providing insight into high-energy intermediates formed during the acid- and base-catalyzed reactions. An experimentally determined value for the hydrolysis of methyl acetate reported a Gibbs free energy of +2.50 kJ/mol; however, this was an acid-catalyzed study [79]. The non-acid-catalyzed computed free energy (Table 2) is larger but also positive and consistent with both the T1 and G3(MP2) calculated values. A study by Shi et al. [80] computed (HF/3-21G level with the Onsager water model) a Gibbs free energy of +4.04 kcal/mol (+16.90 kJ/mol) for the neutral hydrolysis of methyl acetate, which is consistent with the value of +21.70 kJ/mol obtained employing a higher level of theory in our current study (Table 2).

The transition states for hydrolysis and aminolysis of anhydrides [74,81,82], acyl halides [74,83,84], and thioesters [85] have also been studied computationally. The reaction of methylamine with acetic anhydride in the gas phase has been modeled [81] at three levels: RHF/6-31+G(d,p)//RHF/6-31+G(d,p), B3LYP/6-31+G(d,p)//B3LYP/6-31+G(d,p), and MP2/6-31+G(d,p)//MP2/6-31+G(d,p) with  $\Delta E$  energies of  $-89.96$  kJ/mol,  $-88.28$  kJ/mol, and  $-74.48$  kJ/mol, respectively. A value of  $-77.34$  kJ/mol (gas phase) for  $\Delta E$  was obtained in the current study employing the M06-2X/6-311+G(2df,2p)//B3LYP/6-31G(d) level of theory (Table 2). In the case of acetyl chloride, a  $\Delta G = -73.9$  kJ/mol was computed in the water phase at the B3LYP/6-31G(d) level employing the IEF-PCM polarizable continuum model (value extracted from Scheme 2 in Ruff and Farkas [83]) but modeled with a single water molecule adduct for the transition state intermediate.

**Table 2.** M06-2X/6-311+G(2df,2p)//B3LYP/6-31G(d) energies for reaction of water and methylamine with example esters, anhydrides, acetyl chloride, and thioesters.

Reaction	Gas Phase (kJ/mol)	Water (kJ/mol)
 <chem>CC(=O)OC + O &gt;&gt; CC(=O)O + CO</chem>	15.04 ( $\Delta E$ ) 19.26 ( $\Delta G$ ) 18.74 ( $\Delta H$ )	16.42 ( $\Delta E$ ) 21.70 ( $\Delta G$ ) 20.11 ( $\Delta H$ )
 <chem>CC(=O)OC + CN &gt;&gt; CC(=O)NC + CO</chem>	$-3.16$ ( $\Delta E$ ) $-4.25$ ( $\Delta G$ ) $-3.81$ ( $\Delta H$ )	$-19.63$ ( $\Delta E$ ) $-20.73$ ( $\Delta G$ ) $-20.28$ ( $\Delta H$ )
 <chem>CC(=O)OC(=O)C + O &gt;&gt; CC(=O)O + CC(=O)O</chem>	$-54.65$ ( $\Delta E$ ) $-55.85$ ( $\Delta G$ ) $-46.34$ ( $\Delta H$ )	$-47.55$ ( $\Delta E$ ) $-49.83$ ( $\Delta G$ ) $-40.20$ ( $\Delta H$ )
 <chem>CC(=O)OC(=O)C + CN &gt;&gt; CC(=O)NC + CC(=O)O</chem>	$-77.34$ ( $\Delta E$ ) $-85.40$ ( $\Delta G$ ) $-74.34$ ( $\Delta H$ )	$-92.15$ ( $\Delta E$ ) $-98.13$ ( $\Delta G$ ) $-88.83$ ( $\Delta H$ )
 <chem>CC(=O)Cl + O &gt;&gt; CC(=O)O + Cl</chem>	$-43.74$ ( $\Delta E$ ) $-41.72$ ( $\Delta G$ ) $-45.17$ ( $\Delta H$ )	$-37.94$ ( $\Delta E$ ) $-35.92$ ( $\Delta G$ ) $-39.37$ ( $\Delta H$ )
 <chem>CC(=O)Cl + CN &gt;&gt; CC(=O)NC + Cl</chem>	$-61.99$ ( $\Delta E$ ) $-58.07$ ( $\Delta G$ ) $-68.19$ ( $\Delta H$ )	$-74.08$ ( $\Delta E$ ) $-71.01$ ( $\Delta G$ ) $-80.35$ ( $\Delta H$ )
 <chem>CC(=O)S + O &gt;&gt; CC(=O)O + CS</chem>	$-17.17$ ( $\Delta E$ ) $-26.96$ ( $\Delta G$ ) $-15.46$ ( $\Delta H$ )	$-10.03$ ( $\Delta E$ ) $-19.81$ ( $\Delta G$ ) $-8.32$ ( $\Delta H$ )
 <chem>CC(=O)S + CN &gt;&gt; CC(=O)NC + CS</chem>	$-35.41$ ( $\Delta E$ ) $-43.31$ ( $\Delta G$ ) $-38.48$ ( $\Delta H$ )	$-46.19$ ( $\Delta E$ ) $-59.97$ ( $\Delta G$ ) $-48.79$ ( $\Delta H$ )

Thioesters are intermediates in native chemical ligation, intein splicing, and expressed protein ligation strategies in protein engineering [86]. They are also present in certain

cellular metabolic intermediates [87], although bioconjugation reagents based on thioesters are not frequently employed. Cellular thioesters such as acetyl-S-CoA, for example, are substrates for acyltransferase enzymes in cells [87]. However, thioester intermediates can also non-enzymatically acylate cellular proteins in an uncontrolled manner, and this aspect of thioesters will be discussed in a subsequent section (Section 3.4.1) [61,88,89], and hence computed free energy values for their reaction with amino acid side chains can have critically important predictive value to biochemists. Values for the T1 and G3(MP2) energies (gas phase) for reactions of a simple thioester, methyl thioacetate, with H<sub>2</sub>O and with methylamine are provided in Table 1.  $\Delta G$  values for the overall reaction of methyl thioacetate with H<sub>2</sub>O and with methylamine were computed to be  $-19.81$  kJ/mol and  $-59.97$  kJ/mol, respectively, at the M06-2X/6-311+G(2df,2p)//B3LYP/6-31G(d) level (C-PCM intrinsic water phase) (Table 2). The  $\Delta G^\circ$  value for the hydrolysis of a similar thioester, ethyl thioacetate, under standard state conditions (25 °C; 1 M for solutes (with an infinitely diluted reference state) in pure liquid water)) has been reported as  $-4.1 \pm 1.5$  kcal/mol ( $-17.15 \pm 6.28$  kJ/mol) [90]. The experimentally determined free energy for the hydrolysis of another thioester, N,S-diacetyl- $\beta$ -mercaptoethylamine, was reported as  $-4.46$  kcal/mol ( $-18.66$  kJ/mol) [91]. The computed value (C-PCM intrinsic aqueous phase) in the current study for the hydrolysis of methyl thioacetate is  $-19.81$  kJ/mol (Table 2) and is in reasonable agreement with the experimentally obtained values for these types of thioesters. Activation energies have been computed employing transition state models for the reaction of methyl acetate and methyl thioacetate with hydroxide, ammonia, and the carbanion of methyl cyanoacetate to better understand the relative reactivities of oxoesters and thioesters with various nucleophiles. It was found that oxoesters and thioesters have similar reactivity with hydroxide as a nucleophile, but thioesters are 100-fold more reactive toward amine nucleophiles [76]. The free energies of the reaction of thioacetic acid and methyl thioacetate with hydroxide and H<sub>2</sub>O under select pH and temperature conditions were computed at the DFT level (B3LYP//6-31G(d)) and employed in a discussion of the plausibility of these compounds accumulating in various geological environments [85].

### 3.1.2. Phenyl and N-hydroxysuccinimide Esters

Phenyl-based esters compose an important class of bioconjugation reagents and are extensively employed in biochemistry and materials science [4,92,93]. These include *p*-nitrophenyl and fluorinated esters. Tables S1 and S2 provide the computed T1 and G3(MP2) gas phase energies for the hydrolysis and aminolysis reactions for phenyl acetate (5), *p*-nitrophenol acetate (6), and various fluorinated phenyl esters (compounds 7–13), and Table 3 provides the gas phase and aqueous phase thermodynamic values for these esters at the M06-2X/6-311+G(2df,2p)//B3LYP/6-31G(d) level. The amine reactions are more thermodynamically favorable than the attack of water, although these esters are also subject to hydrolysis in aqueous solutions when employed to modify biomolecules in solution [4]. The tetra- and pentafluorophenyl-based esters (compounds of types 12 and 13) are currently preferred modification reagents due to their increased stability in aqueous solutions compared to N-hydroxysuccinimide (NHS) esters (compounds of structure 14 and 15; Table 4). NHS esters have a  $t_{1/2}$  of approximately 5 h at pH 7.0 (0 °C) [94] but only 10 min at pH 8.6 (4 °C) [95]. From Table 3 the *p*-nitrophenyl ester 6 in aqueous media has a thermodynamically more favorable reaction ( $\Delta G = -61.89$  kJ/mol) with amines than the simple phenyl ester 5 ( $\Delta G = -49.72$  kJ/mol) and is much greater than the simple methyl ester 1 (Table 2,  $\Delta G = -20.73$  kJ/mol). It is also interesting to note that a thioester such as compound 4 has a comparable free energy for reaction (Table 2;  $\Delta G = -59.97$  kJ/mol) with amines as the *p*-nitrophenyl esters do, a point to note as we discuss thioester reactions in cells later in this article. The trend within the fluorinated phenyl esters is for increasing fluorination to favor reaction thermodynamics, with the tetrafluoro- and pentafluorophenyl esters having comparable free energies of reactions with methylamine to those of the *p*-nitrophenyl leaving group. Reactions of phenyl [96–100], *p*-nitrophenyl [84,93,98,101], and fluorophenyl esters [92,93] have been studied experimentally and computationally

with various nucleophiles and solvents, with a focus on the transition state structures. For example, a theoretical study of the aminolysis of *para*-substituted phenyl acetates in vacuo and in acetonitrile was undertaken at the B3LYP/6-31+G(d,p) level of theory, and for the reaction of phenyl acetate with ammonia, a reaction energy ( $\Delta E$ ) of  $-13.09$  kcal/mol ( $-54.77$  kJ/mol) was computed. The current study employing methylamine as a nucleophile (Table 3) computed a reaction energy ( $\Delta E$ ) of  $-54.90$  kJ/mol.

**Table 3.** M06-2X/6-311+G(2df,2p)//B3LYP/6-31G(d) energies for reaction of water and methylamine with example phenyl esters.

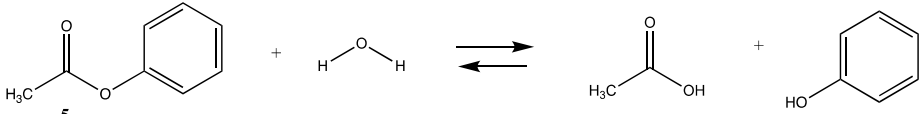
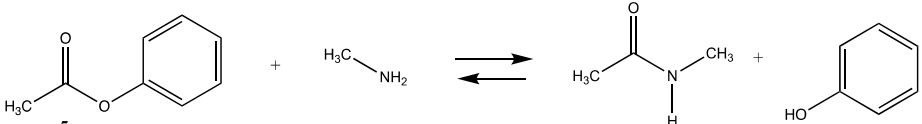
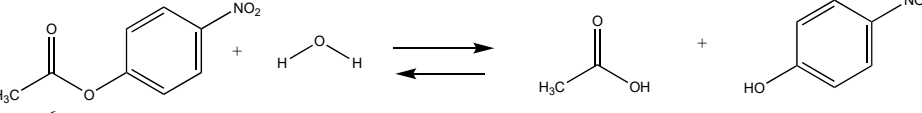
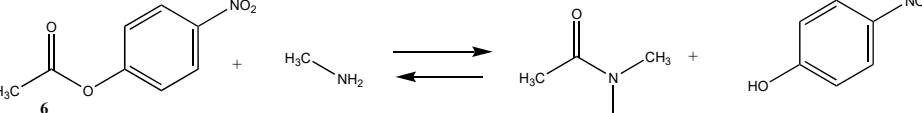
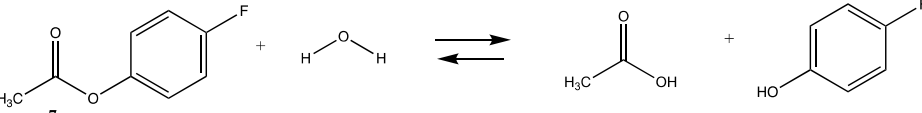
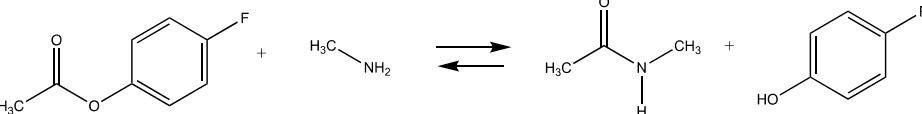
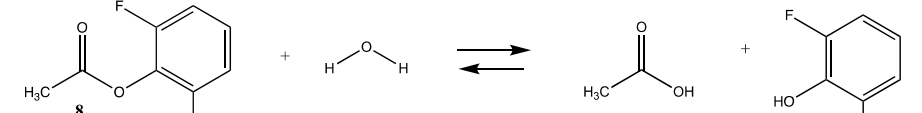
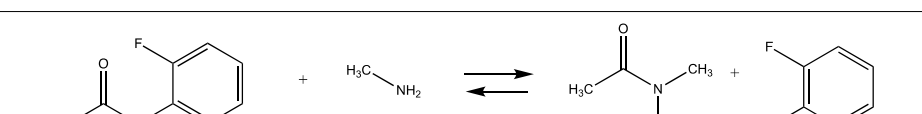
Reaction		Gas Phase (kJ/mol)	Water (kJ/mol)
		$-17.88$ ( $\Delta E$ ) $-14.68$ ( $\Delta G$ ) $-12.18$ ( $\Delta H$ )	$-18.79$ ( $\Delta E$ ) $-15.49$ ( $\Delta G$ ) $-13.08$ ( $\Delta H$ )
		$-36.13$ ( $\Delta E$ ) $-31.03$ ( $\Delta G$ ) $-35.20$ ( $\Delta H$ )	$-54.90$ ( $\Delta E$ ) $-49.72$ ( $\Delta G$ ) $-53.96$ ( $\Delta H$ )
		$-25.68$ ( $\Delta E$ ) $-25.75$ ( $\Delta G$ ) $-18.69$ ( $\Delta H$ )	$-27.60$ ( $\Delta E$ ) $-27.67$ ( $\Delta G$ ) $-20.62$ ( $\Delta H$ )
		$-43.93$ ( $\Delta E$ ) $-42.10$ ( $\Delta G$ ) $-41.71$ ( $\Delta H$ )	$-63.71$ ( $\Delta E$ ) $-61.89$ ( $\Delta G$ ) $-61.50$ ( $\Delta H$ )
		$-15.19$ ( $\Delta E$ ) $-11.16$ ( $\Delta G$ ) $-9.42$ ( $\Delta H$ )	$-17.30$ ( $\Delta E$ ) $-12.94$ ( $\Delta G$ ) $-11.46$ ( $\Delta H$ )
		$-33.44$ ( $\Delta E$ ) $-27.51$ ( $\Delta G$ ) $-32.43$ ( $\Delta H$ )	$-53.41$ ( $\Delta E$ ) $-47.16$ ( $\Delta G$ ) $-52.35$ ( $\Delta H$ )
		$-21.21$ ( $\Delta E$ ) $-20.56$ ( $\Delta G$ ) $-14.48$ ( $\Delta H$ )	$-17.25$ ( $\Delta E$ ) $-16.59$ ( $\Delta G$ ) $-10.52$ ( $\Delta H$ )
		$-39.46$ ( $\Delta E$ ) $-36.91$ ( $\Delta G$ ) $-37.50$ ( $\Delta H$ )	$-53.36$ ( $\Delta E$ ) $-50.82$ ( $\Delta G$ ) $-51.4$ ( $\Delta H$ )

Table 3. Cont.

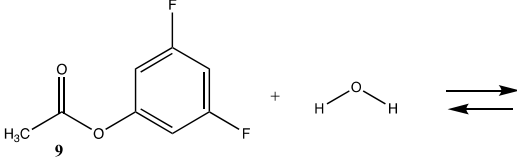
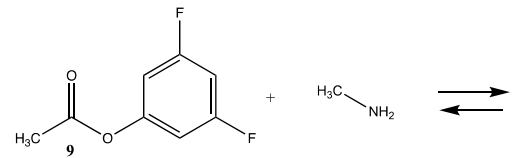
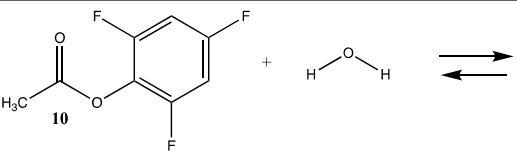
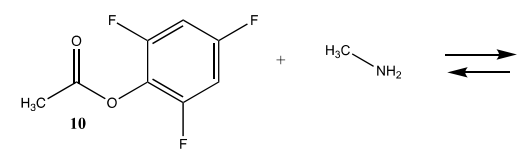
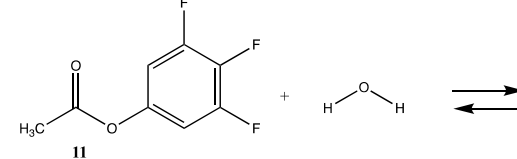
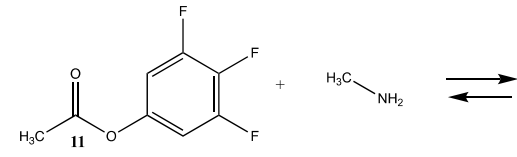
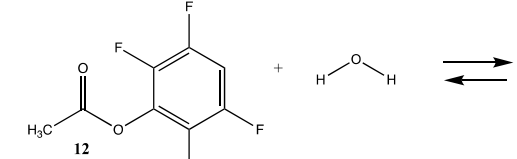
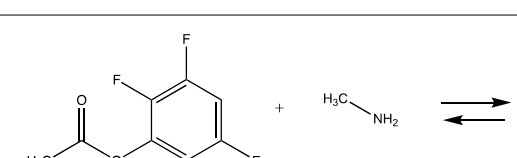
Reaction		Gas Phase (kJ/mol)	Water (kJ/mol)
		−23.23 (ΔE) −20.91 (ΔG) −16.26 (ΔH)	−22.50 (ΔE) −20.50 (ΔG) −15.57 (ΔH)
		−41.48 (ΔE) −37.26 (ΔG) −39.27 (ΔH)	−58.62 (ΔE) −54.73 (ΔG) −56.45 (ΔH)
		−18.28 (ΔE) −19.27 (ΔG) −11.64 (ΔH)	−15.74 (ΔE) −16.72 (ΔG) −9.09 (ΔH)
		−36.48 (ΔE) −43.13 (ΔG) −34.48 (ΔH)	−51.82 (ΔE) −54.68 (ΔG) −49.33 (ΔH)
		−20.56 (ΔE) −20.62 (ΔG) −13.94 (ΔH)	−21.01 (ΔE) −20.67 (ΔG) −14.41 (ΔH)
		−38.76 (ΔE) −44.47 (ΔG) −36.78 (ΔH)	−57.16 (ΔE) −59.27 (ΔG) −54.78 (ΔH)
		−23.72 (ΔE) −24.67 (ΔG) −16.87 (ΔH)	−22.05 (ΔE) −22.53 (ΔG) −15.19 (ΔH)
		−41.95 (ΔE) −47.41 (ΔG) −39.51 (ΔH)	−58.20 (ΔE) −61.14 (ΔG) −55.56 (ΔH)

Table 3. Cont.

Reaction	Gas Phase (kJ/mol)	Water (kJ/mol)
	−20.57 (ΔE) −23.08 (ΔG) −13.89 (ΔH)	−20.57 (ΔE) −22.56 (ΔG) −13.84 (ΔH)
	−38.80 (ΔE) −45.82 (ΔG) −36.53 (ΔH)	−56.72 (ΔE) −61.16 (ΔG) −54.20 (ΔH)

Table 4. M06-2X/6-311+G(2df,2p)//B3LYP/6-31G(d) energies for reaction of water and methylamine with example N-hydroxysuccinimide esters.

Reaction	Gas Phase (kJ/mol)	Water (kJ/mol)
	−6.53 (ΔE) −7.48 (ΔG) 0.28 (ΔH)	−4.21 (ΔE) −4.94 (ΔG) 2.68 (ΔH)
	−24.78 (ΔE) −23.84 (ΔG) −22.74 (ΔH)	−40.37 (ΔE) −39.15 (ΔG) −38.19 (ΔH)
	−7.58 (ΔE) −6.84 (ΔG) −1.77 (ΔH)	−6.06 (ΔE) −5.32 (ΔG) −0.25 (ΔH)
	−25.83 (ΔE) −23.19 (ΔG) −24.78 (ΔH)	−41.82 (ΔE) −39.19 (ΔG) −40.78 (ΔH)

N-hydroxysuccinimide (NHS) and the sulfonated analog esters are also frequently employed in the labeling of lysine residues or peptide/protein immobilization onto surfaces [11,26,102,103] and a wide range of commercial NHS-activated esters are available to researchers (and generally less costly compared to fluorophenyl-activated esters) [3,4]. T1 and G3(MP2) energetics for the reaction of NHS and its sulfonated analog (results in increased water solubility) are presented in Table S3. Table 4 contains the M06-2X/6-311+G(2df,2p)//B3LYP/6-31G(d) level calculations both in the gas phase and in the water phase. There is no calculated difference in favorability between NHS and its sulfonated analog other than the experimental observation that sulfonation enhances the water solubility of molecules attached to the sulfo-NHS moiety and was developed for this reason [4,104]. The ΔG values for the reactions of the NHS (14) and the sulfo-NHS (15) esters of acetic acid with methylamine, as seen from Table 4, are comparable to those of a thioester (Table 2) but less favorable than the fluorinated phenyl esters (Table 3). A computational and mass spectrometric study of the reaction of the sulfo-NHS ester of benzoic acid with primary amines

and guanidine groups in the gas phase has been reported and employed DFT calculations at the B3LYP/6-311G++(d,p) level to elucidate the energies of gas phase complexes [105].

### 3.1.3. Carbonates, Isocyanates, and Isothiocyanates

Carbonates, especially NHS or *p*-nitrophenyl activated carbonates, have been successfully employed in bioconjugation reactions such as crosslinking reactions, for the addition of polyethylene glycol (PEG) to proteins, and for protein immobilization [17,106,107]. Table S4 provides the T1 and G3(MP2) energetics for the reaction of the unactivated carbonate, dimethyl carbonate (16), and the activated carbonates: N-hydroxysuccinimide methyl carbonate (17), and *p*-nitrophenyl methyl carbonate (18) to form the corresponding carbonates. Table 5 provides both the gas phase and water phase thermodynamic values at the M06-2X/6-311+G(2df,2p)//B3LYP/6-31G(d) level. As with the *p*-nitrophenyl ester (6) and the NHS ester (14), the *p*-nitrophenyl carbonate 18 has a more favorable Gibbs free energy in intrinsic water for reaction with methylamine (−76.11 kJ/mol) than the NHS carbonate (17) (−53.28 kJ/mol), although both are highly negative in magnitude and in fact greater than their corresponding esters. Insights into the transition state intermediates for the hydrolysis and aminolysis reactions of the cyclic carbonates, ethylene and propylene carbonate, at the M06/6-31+G(d,p), B3LYP/6-311++G(d,p), MP2/6-311++G(d,p), and the PBE/TZ2P levels have been reported [108–111].

**Table 5.** M06-2X/6-311+G(2df,2p)//B3LYP/6-31G(d) energies for reaction of water and methylamine with example carbonates.

Reaction		Gas Phase (kJ/mol)	Water (kJ/mol)
		14.36 (ΔE) 12.93 (ΔG) 17.9 (ΔH)	15.21 (ΔE) 13.78 (ΔG) 18.75 (ΔH)
		−16.30 (ΔE) −21.36 (ΔG) −17.51 (ΔH)	−23.31 (ΔE) −28.55 (ΔG) −24.69 (ΔH)
		−15.43 (ΔE) −12.89 (ΔG) −9.04 (ΔH)	−14.31 (ΔE) −12.58 (ΔG) −8.29 (ΔH)
		−45.89 (ΔE) −47.63 (ΔG) −44.56 (ΔH)	−52.83 (ΔE) −53.28 (ΔG) −51.48 (ΔH)
		−27.58 (ΔE) −30.84 (ΔG) −20.93 (ΔH)	−31.78 (ΔE) −35.22 (ΔG) −25.18 (ΔH)
		−58.05 (ΔE) −63.91 (ΔG) −56.11 (ΔH)	−70.42 (ΔE) −76.11 (ΔG) −68.40 (ΔH)

Although not employed as frequently as NHS or fluorophenyl esters, isocyanates and isothiocyanates have been used in the bioconjugation and dye labeling of proteins [112–115]. Table S5 summarizes the T1 and G3(MP2) gas phase values for the reaction of H<sub>2</sub>O and methylamine with methyl isocyanate (19), phenyl isocyanate (20), methyl isothiocyanate (21), and phenyl isothiocyanate (22) to form the corresponding ureas and thioureas. Table 6 presents the computed M06-2X/6-311+G(2df,2p)//B3LYP/6-31G(d) level values in both

gas and intrinsic aqueous phases. Although methyl isocyanate and methyl isothiocyanate have approximately the same Gibbs free energy for the reaction with methylamine in water ( $\Delta G = -59.39$  kJ/mol and  $\Delta G = -60.29$  kJ/mol, respectively), phenyl isocyanate (**20**) has a more favorable Gibbs free energy for the reaction with methylamine than that calculated for phenyl isothiocyanate (**22**) ( $\Delta G = -75.48$  kJ/mol and  $\Delta G = -53.16$  kJ/mol, respectively). A DFT investigation (B3LYP/6-311++G(d,p) with the C-PCM intrinsic water model) has been reported on the catalytic effects of water clusters on the hydrolysis of toluene-2,4-diisocyanate. It was concluded that the hydrolysis of 2,4-TDI is hugely accelerated by water molecules acting as the proton conduit by forming hydrogen-bonded ring transition states in the computed mechanism [116].

**Table 6.** M06-2X/6-311+G(2df,2p)//B3LYP/6-31G(d) energies for reaction of water and methylamine with example isocyanates and isothiocyanates.

Reaction		Gas Phase (kJ/mol)	Water (kJ/mol)
		-107.59 ( $\Delta E$ ) -43.88 ( $\Delta G$ ) -94.78 ( $\Delta H$ )	-100.33 ( $\Delta E$ ) -36.62 ( $\Delta G$ ) -87.52 ( $\Delta H$ )
		-110.34 ( $\Delta E$ ) -48.79 ( $\Delta G$ ) -104.15 ( $\Delta H$ )	-121.49 ( $\Delta E$ ) -59.39 ( $\Delta G$ ) -113.27 ( $\Delta H$ )
		-108.46 ( $\Delta E$ ) -51.20 ( $\Delta G$ ) -95.44 ( $\Delta H$ )	-103.03 ( $\Delta E$ ) -45.76 ( $\Delta G$ ) -90.01 ( $\Delta H$ )
		-114.32 ( $\Delta E$ ) -61.84 ( $\Delta G$ ) -106.66 ( $\Delta H$ )	-127.76 ( $\Delta E$ ) -75.48 ( $\Delta G$ ) -120.13 ( $\Delta H$ )
		-84.23 ( $\Delta E$ ) -27.27 ( $\Delta G$ ) -71.00 ( $\Delta H$ )	-71.93 ( $\Delta E$ ) -19.17 ( $\Delta G$ ) -58.22 ( $\Delta H$ )
		-99.68 ( $\Delta E$ ) -40.26 ( $\Delta G$ ) -90.44 ( $\Delta H$ )	-114.08 ( $\Delta E$ ) -60.29 ( $\Delta G$ ) -105.58 ( $\Delta H$ )
		-65.37 ( $\Delta E$ ) -9.07 ( $\Delta G$ ) -52.74 ( $\Delta H$ )	-60.63 ( $\Delta E$ ) -6.42 ( $\Delta G$ ) -47.63 ( $\Delta H$ )
		-82.39 ( $\Delta E$ ) -28.24 ( $\Delta G$ ) -75.12 ( $\Delta H$ )	-108.74 ( $\Delta E$ ) -53.16 ( $\Delta G$ ) -100.6 ( $\Delta H$ )

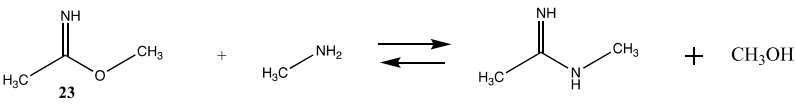
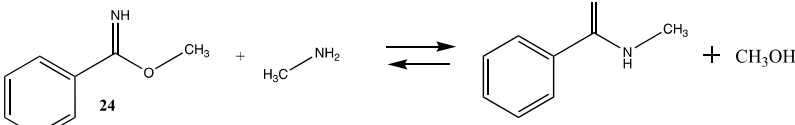
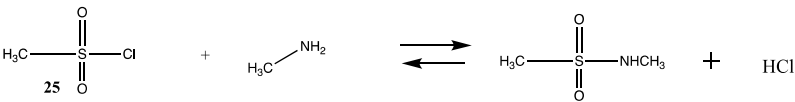
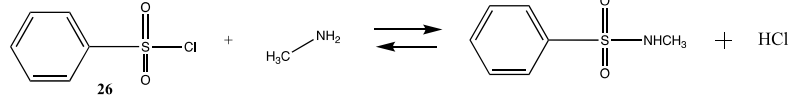
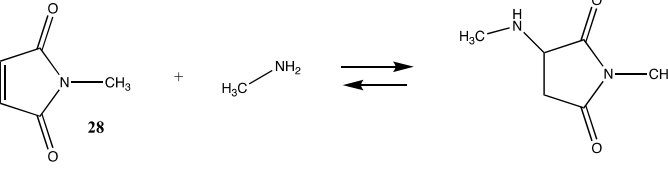
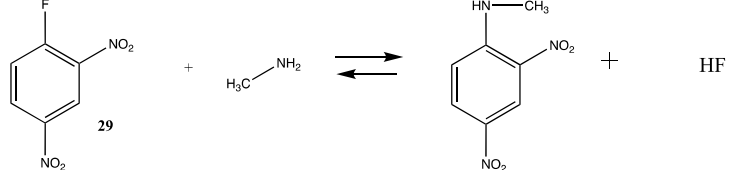
### 3.1.4. Additional Modification Reactions

Other chemical modifications that model the reaction of the side chain of lysine with labeling reagents are surveyed in Tables S6 and S7 and Tables 7 and 8, with T1 and G3(MP2) gas phase results presented in Tables S6 and S7. Methyl acetimidate (**23**) and methyl benzimidate (**24**) are representative of “imidate” modification reagents and react with lysine side chains to produce the corresponding N-methylacetimidamide and N-methylbenzimidamide, respectively. Modest  $\Delta G$  reaction energies (approximately  $-18$  kJ/mol) in water are computed for these reactions (Table 7). Bis-imidate-containing reagents have been employed in protein crosslinking studies to investigate subunit–subunit

as well as protein–protein interactions [3,4,117–119]. Computations on the effects of conjugation on the structures of select imidates have been reported at the B3LYP/6-31G(d) level [120].

Methanesulfonyl chloride (**25**) and phenylsulfonyl chloride (**26**) model sulfonylation reagents can react with the amine moiety in lysine side chains to produce the corresponding sulfonamide products and are employed in the attachment of dyes, such as the sulforhodamines, to proteins for biophysical studies, among other uses [4,121]. These reactions are more favorable than those computed for the imidates (Tables S6 and S7). The Gibbs free energies for the reaction of **25** and **26** with methylamine are highly favorable at  $-43.73$  kJ/mol and  $-51.03$  kJ/mol, respectively. DFT computations on the transition state for hydrolysis of a series of benzenesulfonyl chlorides with seventeen explicit water molecules present in the structure were reported and employed the B3LYP/6-311G(d,p) level after screening a range of functionals and basis sets [122]. Additional studies on the transition state for hydrolysis of various sulfonyl halides have also been reported [123,124].

**Table 7.** M06-2X/6-311+G(2df,2p)//B3LYP/6-31G(d) energies for reaction of methylamine with imidates, sulfonyl chlorides, epoxides, maleimides, and 2,4-dinitrofluorobenzene.

Reaction	Gas Phase (kJ/mol)	Water (kJ/mol)
	-2.39 ( $\Delta E$ ) -4.89 ( $\Delta G$ ) -4.11 ( $\Delta H$ )	-15.16 ( $\Delta E$ ) -17.65 ( $\Delta G$ ) -16.88 ( $\Delta H$ )
	-6.63 ( $\Delta E$ ) -6.95 ( $\Delta G$ ) -7.26 ( $\Delta H$ )	-17.78 ( $\Delta E$ ) -18.98 ( $\Delta G$ ) -18.45 ( $\Delta H$ )
	-35.49 ( $\Delta E$ ) -36.36 ( $\Delta G$ ) -43.22 ( $\Delta H$ )	-42.86 ( $\Delta E$ ) -43.73 ( $\Delta G$ ) -50.58 ( $\Delta H$ )
	-34.50 ( $\Delta E$ ) -34.85 ( $\Delta G$ ) -42.20 ( $\Delta H$ )	-53.06 ( $\Delta E$ ) -51.03 ( $\Delta G$ ) -59.92 ( $\Delta H$ )
	-120.41 ( $\Delta E$ ) -66.04 ( $\Delta G$ ) -113.51 ( $\Delta H$ )	-116.93 ( $\Delta E$ ) -62.56 ( $\Delta G$ ) -110.02 ( $\Delta H$ )
	-105.01 ( $\Delta E$ ) -46.27 ( $\Delta G$ ) -97.70 ( $\Delta H$ )	-91.93 ( $\Delta E$ ) -34.75 ( $\Delta G$ ) -84.41 ( $\Delta H$ )
	-62.60 ( $\Delta E$ ) -52.69 ( $\Delta G$ ) -64.26 ( $\Delta H$ )	-83.95 ( $\Delta E$ ) -73.96 ( $\Delta G$ ) -85.60 ( $\Delta H$ )

Also having highly favorable thermodynamics is the reaction of an epoxide, such as 2-methyloxirane (**27**), with methylamine, resulting in a computed  $\Delta G$  for the reaction between

**27** and methylamine in water of  $-62.56$  kJ/mol (Tables S6 and S7). Epoxides have been employed in protein crosslinking investigations [18] and in enzyme immobilization onto resins [125]. The strained ring system of the epoxide moiety results in favorable reactions with nucleophilic side chains such as lysine and cysteine (Section 3.2). Investigations on the mechanism and transition state intermediates involved in the hydrolysis of ethylene oxide have been studied at the MP2/6-311++G(d,p), B3LYP/6-311+G(d,p) and M06-2X/6-311++G(d,p) levels [126–128].

Maleimide-based reagents, modeled as N-methylmaleimide (**28**) (Tables 7 and S6), can react with lysine side chains but are more selective to cysteine side chains (Section 3.2), given that pH can be used to maintain the protonated state of lysine side chains yet allow for reaction with the thiol functionality on cysteine [129,130]. The  $\Delta G$  for the overall reaction between **28** and methylamine was computed in intrinsic water to be  $-34.75$  kJ/mol, which is less favorable than the reaction of methylamine with an epoxide.

The reagent 2,4-dinitrofluorobenzene (DNFB; **29**) is frequently employed to label proteins, generally at lysine residues, with an aromatic chromophore and is useful in various biophysical studies as well as a useful reagent to block lysine residues when performing complex chemical modifications on proteins [131,132]. The amine functionality nucleophilically attacks the carbon attached to the fluorine in DNFB, generating a substituted aryl-amine bond. This reaction is thermodynamically very favorable, with a  $\Delta G = -73.96$  in the intrinsic aqueous phase (Table 7). The T1 and G3(MP2) energies for this reaction are provided in Table S6 for reference. The activation energies for the reactions of 1-fluoro-2-nitrobenzene and DNFB with ethanolamine as the nucleophile in various organic solvents have been computed at the B3LYP/6-31G(d) level employing the SM8 solvation model [133,134].

**Table 8.** M06-2X/6-311+G(2df,2p)/B3LYP/6-31G(d) energies for reaction of methylamine with example squarate esters and aldehydes.

Reaction	Gas Phase (kJ/mol)	Water (kJ/mol)
	$-44.02$ ( $\Delta E$ ) $-46.26$ ( $\Delta G$ ) $-44.44$ ( $\Delta H$ )	$-57.84$ ( $\Delta E$ ) $-60.08$ ( $\Delta G$ ) $-58.26$ ( $\Delta H$ )
	$-23.70$ ( $\Delta E$ ) $-25.78$ ( $\Delta G$ ) $-25.03$ ( $\Delta H$ )	$-44.02$ ( $\Delta E$ ) $-46.10$ ( $\Delta G$ ) $-45.35$ ( $\Delta H$ )
	$-12.05$ ( $\Delta E$ ) $-9.55$ ( $\Delta G$ ) $-15.37$ ( $\Delta H$ )	$-16.64$ ( $\Delta E$ ) $-14.41$ ( $\Delta G$ ) $-19.91$ ( $\Delta H$ )
	$-3.47$ ( $\Delta E$ ) $-2.3$ ( $\Delta G$ ) $-9.8$ ( $\Delta H$ )	$-9.67$ ( $\Delta E$ ) $-8.51$ ( $\Delta G$ ) $-15.98$ ( $\Delta H$ )

Squaric acid esters, such as dimethyl squarate (**30**), can react with amines to form mono-squaramide (**31**) and can react further with a second amine to form bis-squaramides [135–138] (Tables 8 and S7). This chemistry has been employed as a mild method to covalently attach

complex molecules to the lysine side chain of proteins. This has included carbohydrates and polyethylene glycol (PEG) chains in proteins [139–142]. Although both reactions are favorable ( $\Delta G = -60.08$  kJ/mol and  $-46.10$  kJ/mol, respectively), the first conjugation is more favorable from a thermodynamic perspective. Once the first amine-containing molecule is attached to **30**, such as an amine-containing fluorophore or PEG group, the remaining alkoxy group can be displaced by an exposed lysine side chain on the surface of a protein, resulting in the attachment of a new molecular entity to the protein. Molecular properties calculated at the B3LYP/6-31G(d,p) level for the bis-squaramide, 3,4-bis(isopropylamino)cyclobut-3-ene-1,2-dione, were reported to agree well with experimental values for the geometry, atomic charges, vibrational frequencies, absorption wavelengths, and the HOMO and LUMO energies [143]. For 1,2-dianilinosquairane, the B3LYP/6-311++G(d,p) level DFT calculations were found to be in agreement with various experimental properties for this compound [144]. The hydrolysis of several mono- and bis-squaramides has been studied at the M06-2X//cc-pVTZ level employing PCM intrinsic aqueous conditions [145].

Modification of the N-terminal amine in proteins as well as the lysine side chain can be accomplished by the formation of a Schiff base with a carbonyl-containing molecule such as an aldehyde [4,131,146]. For example, the reaction of acetaldehyde or benzaldehyde derivatives can form imines with amine nucleophiles, and although these can reversibly dissociate to the starting aldehyde and amine in water, the imines are generally reduced by a further reaction employing a reagent such as sodium borohydride, NaBH<sub>4</sub>, or sodium cyanoborohydride, NaBH<sub>3</sub>CN, to form the alkylated amine, thus stabilizing the carbon-nitrogen bond to hydrolysis [4,131]. Although the initial formation of the imine is not greatly favorable from a thermodynamic perspective ( $\Delta G = -14.41$  kJ/mol and  $-8.51$  kJ/mol) (Tables 8 and S7 for T1 and G3(MP2) values), the subsequent reduction shifts the reaction to the labeled amine. DFT studies on the mechanism of the reaction of acetaldehyde and glycolaldehyde with pyridoxamine employing the B3LYP as well as the M06-2X functionals with the 6-31+G(d) and the 6-31+G(d,p) basis sets have been reported and have provided insight into the structures of the carbinolamine intermediate [147]. Also reported is the application of B3LYP/6-31+G(d) level calculations to study the mechanism of the aldehyde, pyridoxal, with various amines [148].

### 3.2. Cysteine Bioconjugation Reactions

Sulfonyl Chlorides, Epoxides, Maleimides, 2,4-Dinitrofluorobenzene, Disulfides,  $\alpha$ -Bromoacids and  $\alpha$ -Bromoamides

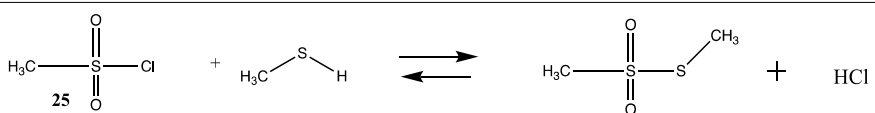
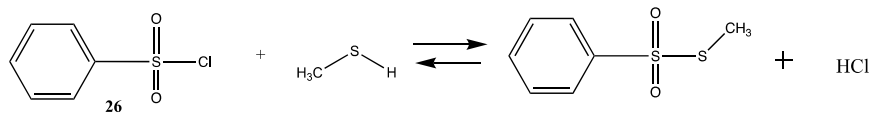
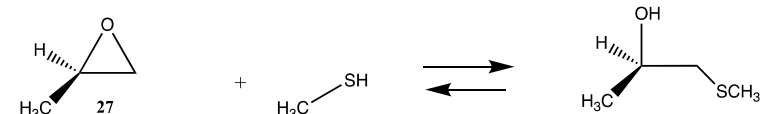
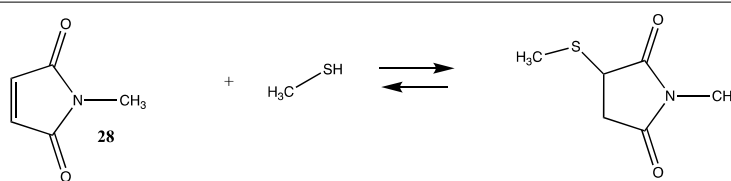
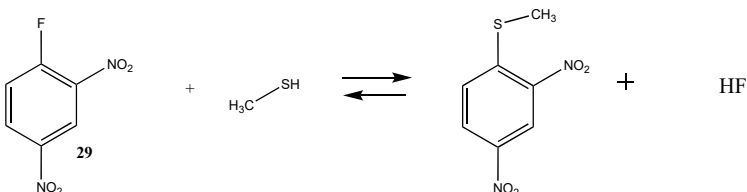
Reagents that target cysteine residues are important, and, due to the low abundance of exposed cysteine surface residues in the majority of proteins [87], site-directed mutagenesis has been a very successful strategy to introduce a surface-exposed cysteine for labeling or for crosslinking studies [13,130,149–151]. The reaction of thiols with epoxides is important in the thiol-epoxy “Click” reaction, allowing for the rapid formation of covalent bonds under mild conditions and having importance in the preparation of hydrogels used in tissue engineering, for example [152,153]. The reaction of sulfonyl chlorides **25** and **26**, 2-methyloxirane (**27**), N-methylmaleimide (**28**), and DNFB (**29**) with methanethiol as a model for the cysteine side chain is presented in Table S8 (T1 and G3(MP2)) and Table 9 (M06-2X/6-311+G(2df,2p)//B3LYP/6-31G(d) in vacuum and intrinsic aqueous phase). The reactions of 2-methyloxirane (**27**) and N-methylmaleimide (**28**) are the most thermodynamically favorable ( $\Delta G$  values of  $-77.84$  kJ/mol and  $-55.92$  kJ/mol, respectively) (Table 9) for the overall reaction with methanethiol in an aqueous phase and comparable to those reagents with the lysine side chain model, methylamine. On the other hand, the methylamine reactions involving the sulfonyl chlorides and DNFB are more thermodynamically favorable compared to the thiol reaction with these molecules (Tables 7 and S6).

Computational studies have been reported for the reaction of methanethiol and an active site cysteine with the epoxide-containing antibiotic, Fosfomycin, at the B3LYP/def2-SVP level to elucidate the reaction mechanism of enzyme inactivation by this antibiotic [154]. An excellent recent theoretical investigation on the addition of methanethiol with over

forty different Michael acceptors, including two maleimides, is available [47]. A value for  $\Delta E$  of  $-27.0$  kcal/mol ( $-112.97$  kJ/mol) for the reaction of methanethiol with **28** at the M06-2X/6-311+G(d,p) level in C-PCM intrinsic water was reported [47]. A value for  $\Delta E$  of  $-111.84$  kJ/mol in C-PCM water was obtained in the current study (Table 9). Activation energies calculated at the MP2/6-31+G(d)//HF/6-31+G(d) level for the reaction of 1-substituted-2,4-dinitrobenzenes with piperidine, dimethylamine, and  $-SH$  have been reported [155]. Additional computational studies of thiols with maleimide to further elucidate reaction mechanisms have been reported as well [156,157].

Thiol–disulfide exchange reactions as well as reactions with alpha-halocarbonyls have also been employed as cysteine labeling strategies [4,9,131]. In the case of thiol–disulfide exchange reactions, the chemical moiety attached to the disulfide reagent is critical to shifting the equilibrium towards labeling the cysteine residue, and 2-thiopyridine (**35**) has been advantageous as the leaving group for these reagents. Modeled here is the reaction of 2-(methylsulfanyl)pyridine (**34**) with methanethiol, as shown in Tables 10 and S9. In fact, the tautomerization of the 2-thiopyridine (**35**) to pyridine-2(1H)-thione (**36**) shifts the thermodynamics of the thiol–disulfide exchange, as can be seen in comparing the free energies for the formation of the disulfide and **35** compared to the formation of compound **36** with  $\Delta G$  values =  $-8.90$  kJ/mol versus  $-31.80$  kJ/mol, respectively. Experimentally, the formation of **36** can be monitored to ascertain the extent of the cysteine labeling reaction [4]. A computational investigation of the equilibrium between **35** and **36** in various solvents employing a diverse set of density functionals and basis sets has been reported, indicating the thermodynamic preference for tautomer **36** [158].

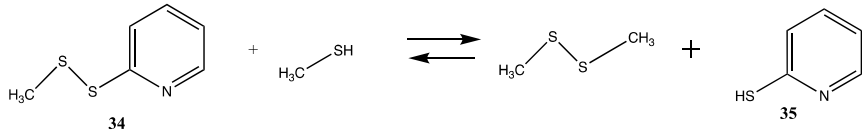
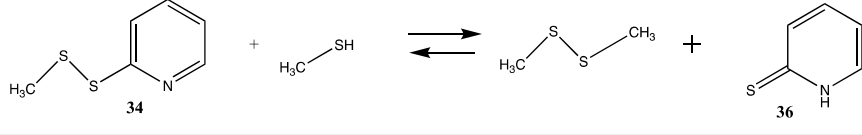
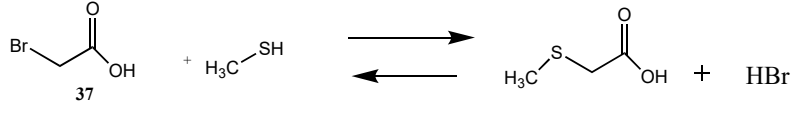
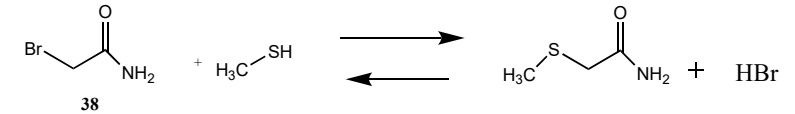
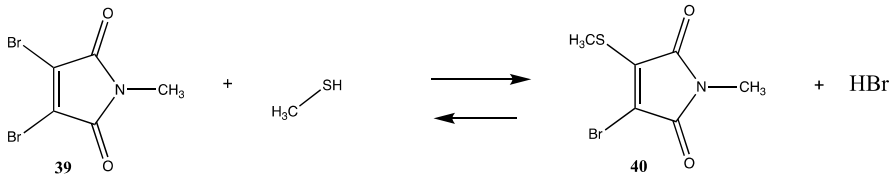
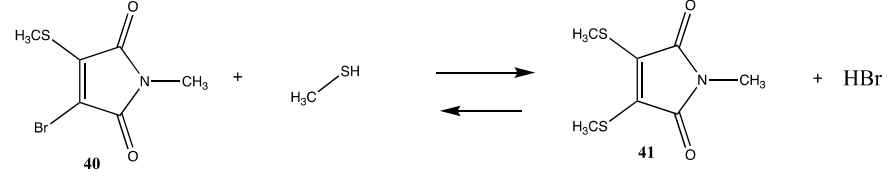
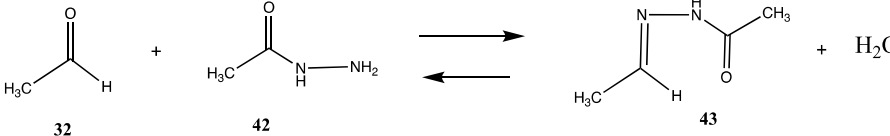
**Table 9.** M06-2X/6-311+G(2df,2p)//B3LYP/6-31G(d) energies for reaction of methanethiol with sulfonyl chlorides, epoxides, maleimides, and 2,4-dinitrofluorobenzene.

Reaction		Gas Phase (kJ/mol)	Water (kJ/mol)
		$-19.34$ ( $\Delta E$ ) $-11.28$ ( $\Delta G$ ) $-22.26$ ( $\Delta H$ )	$-27.45$ ( $\Delta E$ ) $-19.39$ ( $\Delta G$ ) $-30.37$ ( $\Delta H$ )
		$-28.32$ ( $\Delta E$ ) $-24.75$ ( $\Delta G$ ) $-30.8$ ( $\Delta H$ )	$-38.26$ ( $\Delta E$ ) $-34.48$ ( $\Delta G$ ) $-40.50$ ( $\Delta H$ )
		$-134.89$ ( $\Delta E$ ) $-77.60$ ( $\Delta G$ ) $-123.47$ ( $\Delta H$ )	$-135.13$ ( $\Delta E$ ) $-77.84$ ( $\Delta G$ ) $-123.71$ ( $\Delta H$ )
		$-109.96$ ( $\Delta E$ ) $-43.36$ ( $\Delta G$ ) $-98.95$ ( $\Delta H$ )	$-111.84$ ( $\Delta E$ ) $-55.92$ ( $\Delta G$ ) $-101.03$ ( $\Delta H$ )
		$-36.56$ ( $\Delta E$ ) $-26.20$ ( $\Delta G$ ) $-35.74$ ( $\Delta H$ )	$-46.04$ ( $\Delta E$ ) $-35.59$ ( $\Delta G$ ) $-44.95$ ( $\Delta H$ )

Alkylation of cysteine side chains with  $\alpha$ -halocarbonyls such as  $\alpha$ -bromoacetic acid (**37**) and  $\alpha$ -bromoacetamide (**38**) produces the thioether modification on the cysteine side

chain [3,4,159]. The T1, G3(MP2) and M06-2X/6-311+G(2df,2p)//B3LYP/6-31G(d) thermodynamic values are found in Tables 10 and S9, respectively. The choice of the carbonyl group attached to the halide can alter the selectivity of alkylation [160,161]. For example, some proteins may be alkylated only by 37 or 38 [162].

**Table 10.** M06-2X/6-311+G(2df,2p)//B3LYP/6-31G(d) energies for reaction of methanethiol with examples of disulfides,  $\alpha$ -bromoacids and  $\alpha$ -bromoamides, dibromomaleimides, and reaction of acetaldehyde with N-acetylhydrazide.

Reaction		Gas Phase (kJ/mol)	Water (kJ/mol)
		−5.41 ( $\Delta E$ ) −8.27 ( $\Delta G$ ) −4.53 ( $\Delta H$ )	−6.04 ( $\Delta E$ ) −8.90 ( $\Delta G$ ) −5.16 ( $\Delta H$ )
		−11.42 ( $\Delta E$ ) −3.03 ( $\Delta G$ ) −1.46 ( $\Delta H$ )	−40.19 ( $\Delta E$ ) −31.80 ( $\Delta G$ ) −30.24 ( $\Delta H$ )
		−17.63 ( $\Delta E$ ) −16.47 ( $\Delta G$ ) −22.03 ( $\Delta H$ )	−22.70 ( $\Delta E$ ) −18.64 ( $\Delta G$ ) −25.60 ( $\Delta H$ )
		−20.21 ( $\Delta E$ ) −14.59 ( $\Delta G$ ) −24.44 ( $\Delta H$ )	−22.15 ( $\Delta E$ ) −16.19 ( $\Delta G$ ) −25.16 ( $\Delta H$ )
		−43.49 ( $\Delta E$ ) −36.36 ( $\Delta G$ ) −46.60 ( $\Delta H$ )	−43.97 ( $\Delta E$ ) −36.84 ( $\Delta G$ ) −47.08 ( $\Delta H$ )
		−32.88 ( $\Delta E$ ) −26.76 ( $\Delta G$ ) −37.22 ( $\Delta H$ )	−32.06 ( $\Delta E$ ) −25.79 ( $\Delta G$ ) −36.24 ( $\Delta H$ )
		−23.65 ( $\Delta E$ ) −18.70 ( $\Delta G$ ) −28.63 ( $\Delta H$ )	−25.97 ( $\Delta E$ ) −21.02 ( $\Delta G$ ) −30.95 ( $\Delta H$ )

One area of cysteine labeling that has an immense impact on medicine is that of antibody labeling to produce new diagnostics and chemotherapeutics [13,130,163–165]. Attaching anticancer agents to the Fc region of an antibody can allow for the delivery of a chemotherapeutic to cancer cells, reducing off-target toxicities. Although numerous cysteine residues are present in antibodies, they exist in disulfide form as cystines [87]. Controlled reduction, such as with tris (2-carboxyethyl) phosphine (TCEP) or other reductants, can uncover modifiable cysteine side chains, which can then be modified with a variety of molecules [4,130]. Dibromomaleimides are useful cysteine modification reagents as the adjacent pair of cysteine residues generated by controlled reduction on an antibody can be doubly labeled to the same maleimide, providing a more stable linkage to the

antibody [13,130,166–168]. The molecule 2,3-dibromo-N-methylmaleimide (**39**) was chosen as a model for this category of cysteine modification employing methanethiol as a cysteine side chain surrogate (Tables 10 and S9). The overall thermodynamics of the stepwise process to the mono-substituted adduct, **40**, and finally to the disubstituted maleimide, **41**, were computed in the gas phase employing the T1 and G3(MP2) thermochemical recipes as well as at the M06-2X/6-311+G(2df,2p)//B3LYP/6-31G(d) level in the gas phase and in C-PCM intrinsic water (Tables 10 and S9). Both steps are favorable reactions, with  $\Delta G = -36.84$  kJ/mol and  $-25.79$  kJ/mol, respectively (C-PCM water phase), although less so than the reaction with the non-halogenated N-methylmaleimide (**28**) (Table 9). The computed spectroscopic properties for compound **39**, such as infrared and Raman spectra and molecular structure calculated using the B3LYP functional with a range of basis sets, were found to be in good agreement with the experimental properties for this molecule [169].

Although not involving lysine or cysteine bioconjugation, in regards to antibody labeling, another approach that has proven to be useful and should be mentioned is the reaction of an aldehyde generated on the antibody with an acylhydrazide to form the stable acylhydrazone [4,13,165,170]. For computational purposes, this reaction is exemplified by the simple reaction of acetaldehyde (**32**) and acetohydrazide (**42**) to produce E/Z-N<sup>1</sup>-ethylideneacetohydrazide (**43**). Tables 10 and S9 provide the reaction thermodynamics for this adduct formation with  $\Delta G = -21.02$  kJ/mol at the M06-2X/6-311+G(2df,2p)//B3LYP/6-31G(d) level in C-PCM intrinsic water. The aldehyde on the antibody is generated by the periodate oxidation of the carbohydrate present on the antibody. The formed aldehyde can then be reacted with the acylhydrazide. A study on a series of N-acylhydrazone structures and computation of their conformational energies has been reported, which employed a B3LYP/6-31G(d) level approach [171].

The following two figures summarize the computed  $\Delta G$  thermodynamics of the various reactions with methylamine (Figure 2) and methanethiol (Figure 3) as analogs of the lysine and cysteine side chains at the M06-2X/6-311+G(2df,2p)//B3LYP/6-31G(d) level employing C-PCM intrinsic aqueous conditions.

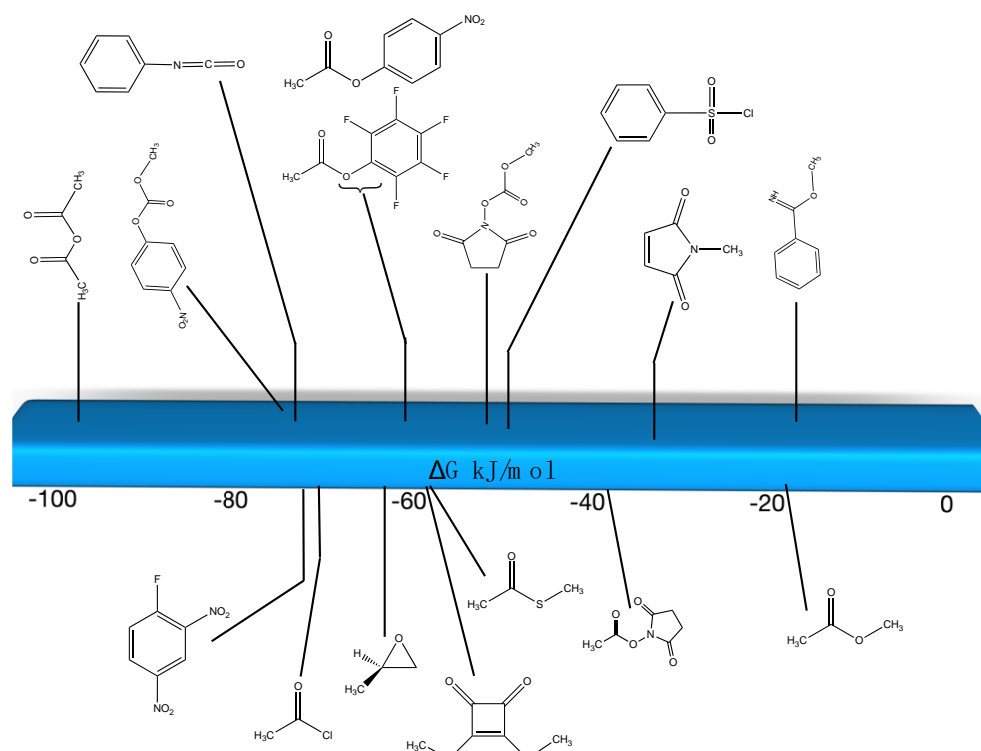


**Figure 2.** Graphical representation of several key bioconjugation reagents and the  $\Delta G$  values computed for their reaction with methylamine at the M06-2X/6-311+G(2df,2p)//B3LYP/6-31G(d) level in water (C-PCM intrinsic solvent model).

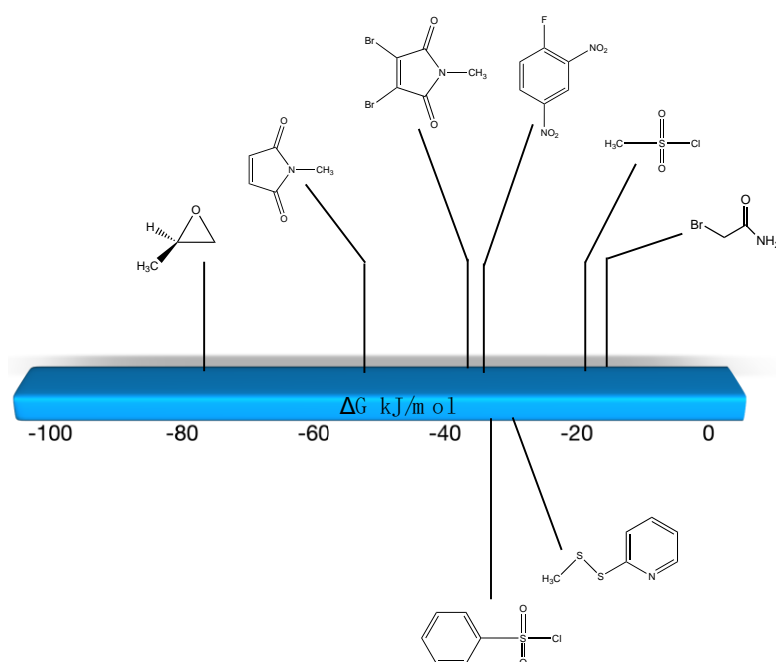


**Figure 3.** Graphical representation of several key bioconjugation reagents and the  $\Delta G$  values computed for their reaction with methanethiol at the M06-2X/6-311+G(2df,2p)//B3LYP/6-31G(d) level in water (C-PCM intrinsic solvent model).

### 3.3. Click Reactions

The term “click” chemistry was introduced by Sharpless and co-workers to categorize chemical reactions that were rapid, facile, and of a general nature [172,173]. Cycloaddition reactions also play an important role in click chemistry-based bioconjugation reactions, although lysine and cysteine side chains are not directly involved in these cycloaddition reactions. However, the introduction of the necessary functional groups (azide or acetylene, for example) may employ site-directed unnatural amino acid incorporation into a protein using molecular biology methods [20,22,23,25,174,175] or employ the previously discussed lysine or cysteine modification chemistries to introduce either the azide or the acetylene onto the protein surface. Given the previously computed conjugation reactions covered in this article, it is interesting to also compute the overall reaction thermodynamics for several representative examples of current click chemistry bioconjugation reactions [170,176–178]. The overall thermodynamics of the reactions of the following model compounds were studied (Tables 11 and S10): methyl azide (44) with (i) propyne (45) to produce triazole 46; (ii) N-acetyl-dibenzoazacyclooctyne (DBCO; 47) to produce triazole 48; and (iii) the bicyclo [6.1.0]non-4-yne (BCN) analog (49) to produce triazole 50; and the reaction of a strained alkene such as trans-cyclooctene (TCO; 51) and a 1,2,4,5-tetrazine such as the model compound 3-methyl-6-phenyl-1,2,4,5-tetrazine (52) to form the 1-methyl-4-phenyl-2,4a,5,6,7,8,9,10-octahydrocycloocta[d]pyridazine (53) adduct and a molecule of nitrogen. The gas phase T1 energies are extremely favorable, as shown in Table S10, and their aqueous reaction thermodynamics at the M06-2X/cc-PVTZ(-f)++ in implicit water are given in Table 11, which are again highly favorable, with the tetrazine reaction being most favorable overall with a  $\Delta G$  of  $-286.65$  kJ/mol. For comparison purposes, the computed reaction thermodynamics at this same level of theory are provided for the reaction of (i) methyl acetate (1) with methyl amine; (ii) S-methyl thioacetate (4) with H<sub>2</sub>O and with methylamine; and (iii) N-methylmaleimide (28) with methanethiol. A range of click chemistry reagents are available commercially that contain maleimide, NHS, or fluorophenyl ester leaving groups, allowing for the introduction of a variety of azides, strained alkynes, or tetrazines into a protein through chemical reactions at lysine or cysteine side chains, as discussed above. A study on the origin of the orthogonality of strain-promoted click reactions at the M06-2X/6-311+G(d,p) with PCM intrinsic solvent has been reported [179]. A recent investigation on

the inverse electron demand Diels–Alder reaction at the M06-2X/6-311+G(d,p) level has also appeared [180]. Additional computational studies providing insight into various click chemistry bioconjugation reactions are available [181–183].

**Table 11.** M06-2X/cc-PVTZ(-f)++ in implicit water energies for benchmark reactions of methylamine, water, and methanethiol with various electrophiles compared to examples of common click reactions.

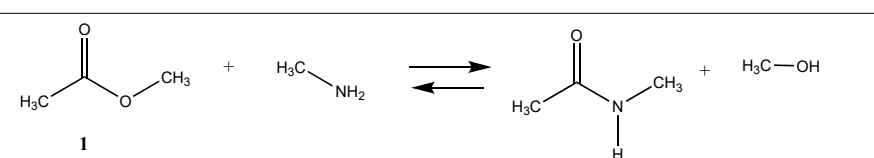
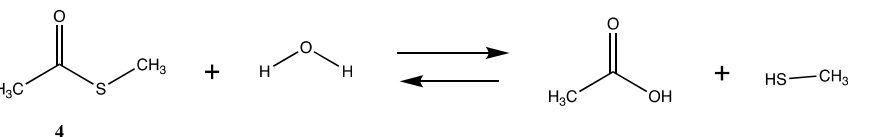
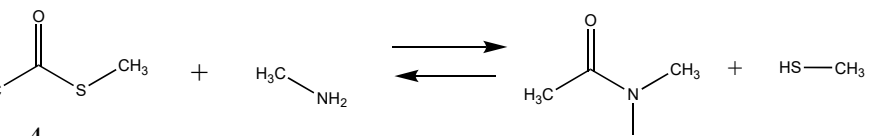
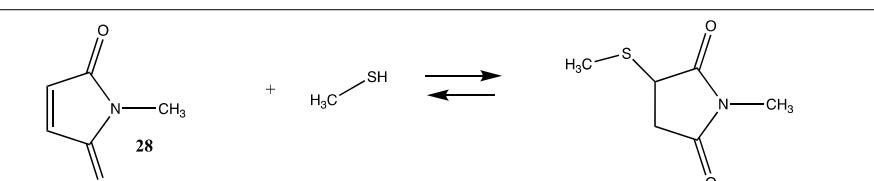
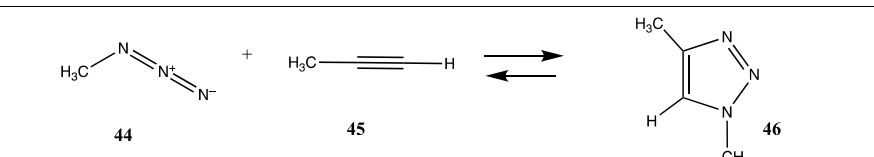
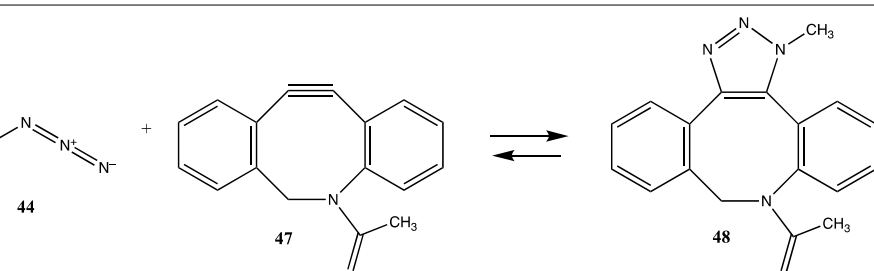
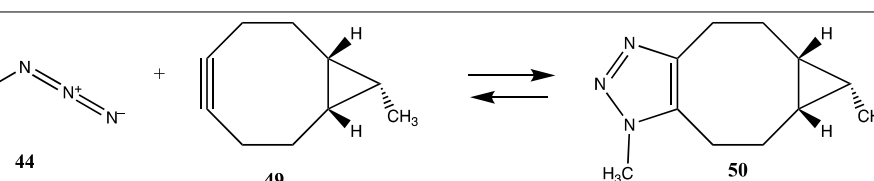
Reaction		M06-2X/cc-PVTZ(-f)++ in Implicit Water (kJ/mol)
 <p>1</p>		−19.54 (ΔE) −22.22 (ΔG) −19.96 (ΔH)
 <p>4</p>		−8.49 (ΔE) −13.81 (ΔG) −9.41 (ΔH)
 <p>4</p>		−44.22 (ΔE) −49.20 (ΔG) −47.91 (ΔH)
 <p>28</p>		−113.68 (ΔE) −44.56 (ΔG) −99.70 (ΔH)
 <p>44</p> <p>45</p> <p>46</p>		−311.29 (ΔE) −238.03 (ΔG) −295.56 (ΔH)
 <p>44</p> <p>47</p> <p>48</p>		−338.61 (ΔE) −259.83 (ΔG) −324.59 (ΔH)
 <p>44</p> <p>49</p> <p>50</p>		−348.32 (ΔE) −269.03 (ΔG) −333.13 (ΔH)

Table 11. Cont.

Reaction		M06-2X/cc-PVTZ(-f)++ in Implicit Water (kJ/mol)
	$\rightleftharpoons$	−310.62 ( $\Delta E$ ) −286.65 ( $\Delta G$ ) −301.33 ( $\Delta H$ )

### 3.4. Reactive Cellular Intermediates

#### 3.4.1. Thioesters, Cyclic Anhydrides, and Acylphosphates

A fascinating aspect of the chemical modification of proteins is the finding that normal cellular molecules and intermediates involved in metabolic pathways can also non-enzymatically label proteins and result in the alteration of cellular biochemistry [88,89,184–187]. Intense interest is being focused on experimental data that show that coenzyme-A (CoA) containing thioester cellular molecules such as succinyl-CoA, an intermediate in the citric acid cycle; glutaryl-CoA, an intermediate in the metabolism of lysine and tryptophan; 3-hydroxy-3-methylglutaryl-CoA (HMG-CoA), an intermediate in the mevalonate and ketogenesis pathways; and 3-methylglutaryl-CoA, a product of leucine catabolic pathway enzyme deficiencies, non-enzymatically label proteins in vivo [32,87–89]. Several other CoA thioesters are also implicated in non-enzymatic protein acylation [188–190]. These acylations have been identified by their presence in many proteins, such as histones and mitochondrial proteins, which may alter their biological activity [189,191–193]. It has also been suggested that these modifications may contribute to the aging process and have contributed to the development of simple metabolic pathways in primordial life [194–200]. Table 12 provides the calculated reaction thermodynamic values for the model reactions of these mentioned reactions, with compound 54 serving as a model for succinyl-CoA, yielding the acylated product 55 with methylamine serving as the lysine side chain; compound 56 serving as a model for glutaryl-CoA, yielding product 57; compound 58 serving as a surrogate of 3-hydroxy-3-methylglutaryl-CoA and producing 59; and compound 60 serving as a model for 3-methylglutaryl-CoA and yielding the N-acylated product 61. The large negative free energy values computed for these model reactions (averaging between  $\Delta G = -58$  and  $-61$  kJ/mol) (Table 12) are clearly consistent with the observed acylation reactions and the identified lysine modifications found by various studies.

It has also been proposed, in addition to the direct non-enzymatic acylation of proteins by thioesters, that their anhydrides, produced by self-cyclization in the cell, also likely contribute to protein modification [30,89,191,201]. The reactions of these corresponding cyclic anhydrides (62, 63, 64, and 65) with methylamine were also computed and are presented in Table 12. Free energy values range between  $-41$  and  $-47$  kJ/mol, although lower than those calculated for the thioesters, are still sufficiently negative in magnitude to favor amine acylation and are consistent with this alternate non-enzymatic acylation pathway in cells. It is interesting to note that a recent publication reviews the use of cyclic anhydrides as important reagents for bioconjugation reactions [64]. In addition, proteins have been identified (reviewed in [30]) that contain 2-butenoyl- and D-lactoyl-modified lysine residues and indicate that 2-butenoyl-CoA and an S-D-lactoyl thioester, modeled as compounds 66 and 67 (Table 12), are also capable of posttranslational protein modifications (PTM) ( $\Delta G$  values of  $-46.9$  kJ/mol and  $-50.5$  kJ/mol, respectively). In the case of the S-D-lactoyl group, S-D-lactoyl-glutathione, a product of the reaction of methylglyoxal with glutathione and catalyzed by the enzyme glyoxalase I [202,203], may be the source for this reactive thioester as well as lactoyl-CoA [30,204].

An obvious additional type of reactive cellular molecule that appears to be involved in non-enzymatic posttranslational modifications would be acyl phosphates, such as acetyl phosphate (**68**) and 1,3-diphosphoglycerate (**69**), both “high energy” intermediates in the glycolytic cycle in cells [33,60,87,184–186,205,206]. These are modeled with methylamine, and free energy values were computed to be  $-33.47$  kJ/mol and  $-63.93$  kJ/mol, respectively. Both are large negative values for reactions with an amine and would be consistent with how these molecules have been reported to contribute to PTM in cells. The larger free energy of reaction of **69** with methylamine compared to **68** may be due to the large repulsive interactions that are present in **69** due to the four negatively charged oxygens at physiological pH. It is interesting to note that Kluger and colleagues have experimentally employed an acyl phosphate, the monomethyl ester of acetyl phosphate, as a targeted acetylation reagent, which further extends the reactivity of acyl phosphates to controllable chemical modification reagents [207–210]. Kataoka and co-workers have observed active site lysine residue acetylation by the above reagent in phenylalanine dehydrogenase [211].

**Table 12.** M06-2X/cc-PVTZ(-f)++ in implicit water energies for methylamine reaction with various models of common cellular intermediates such as thioesters, cyclic anhydrides, acylphosphates, and acetyl-L-carnitine.

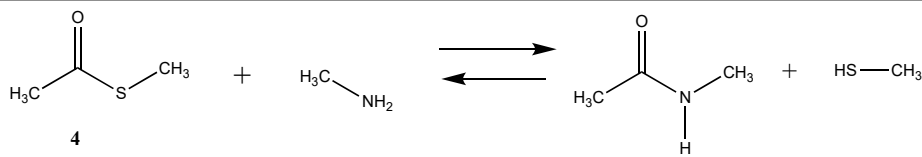
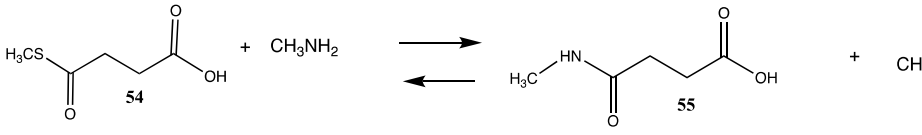
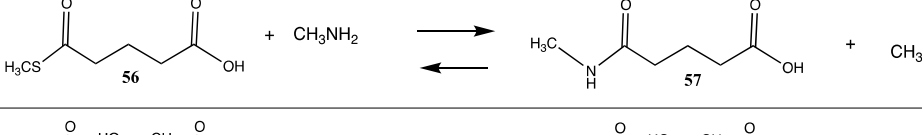
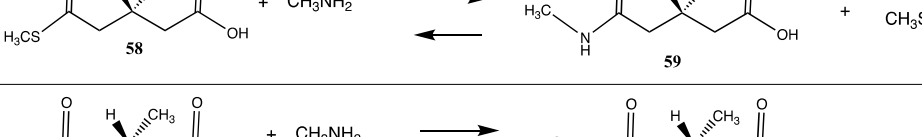
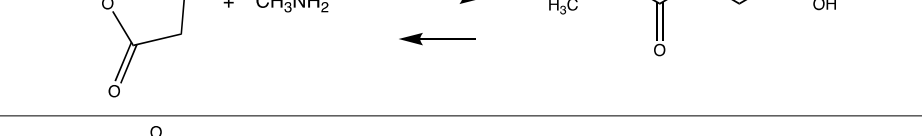
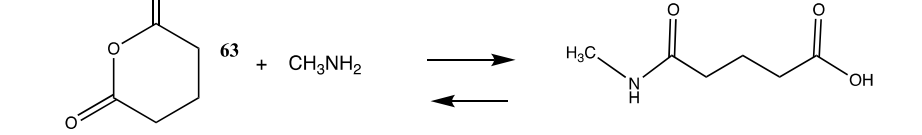
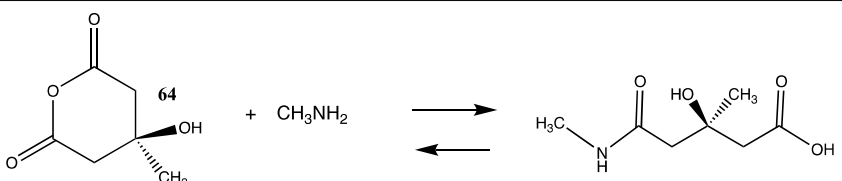
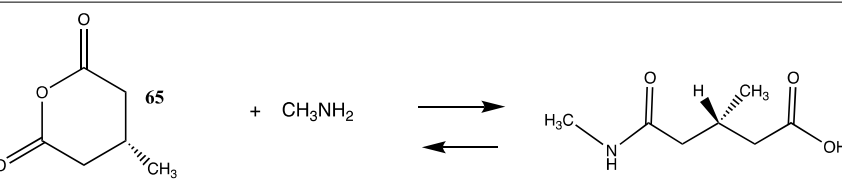
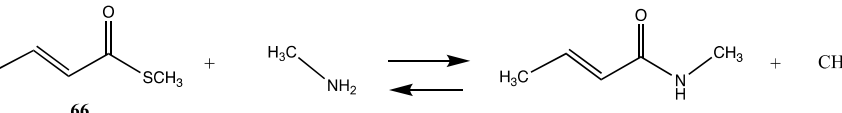
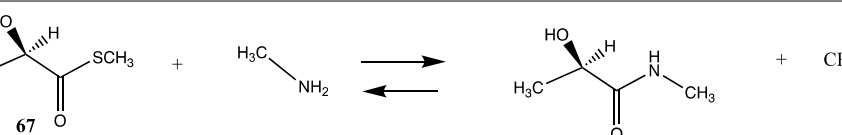
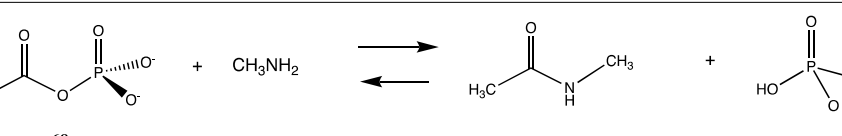
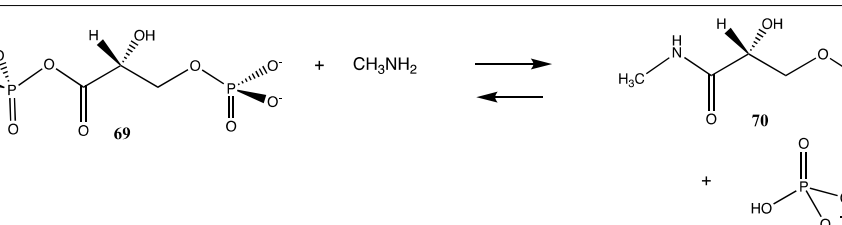
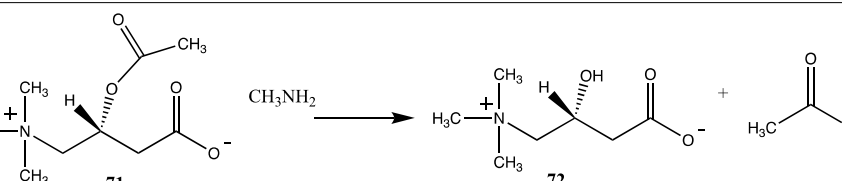
Reaction		M06-2X/cc-PVTZ(-f)++ in Implicit Water (kJ/mol)
		$-44.22$ ( $\Delta E$ ) $-49.20$ ( $\Delta G$ ) $-47.91$ ( $\Delta H$ )
		$-58.32$ ( $\Delta E$ ) $-61.17$ ( $\Delta G$ ) $-62.63$ ( $\Delta H$ )
		$-54.60$ ( $\Delta E$ ) $-58.58$ ( $\Delta G$ ) $-58.99$ ( $\Delta H$ )
		$-54.06$ ( $\Delta E$ ) $-58.62$ ( $\Delta G$ ) $-57.95$ ( $\Delta H$ )
		$-61.09$ ( $\Delta E$ ) $-61.13$ ( $\Delta G$ ) $-63.76$ ( $\Delta H$ )
		$-98.49$ ( $\Delta E$ ) $-41.25$ ( $\Delta G$ ) $-91.09$ ( $\Delta H$ )
		$-105.69$ ( $\Delta E$ ) $-47.24$ ( $\Delta G$ ) $-97.15$ ( $\Delta H$ )

Table 12. Cont.

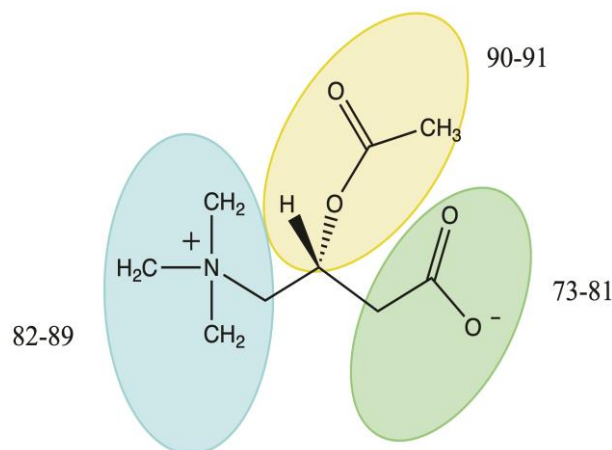
Reaction		M06-2X/cc-PVTZ(-f)++ in Implicit Water (kJ/mol)
		-105.35 ( $\Delta E$ ) -47.66 ( $\Delta G$ ) -97.15 ( $\Delta H$ )
		-104.56 ( $\Delta E$ ) -43.26 ( $\Delta G$ ) -98.28 ( $\Delta H$ )
		-40.67 ( $\Delta E$ ) -46.90 ( $\Delta G$ ) -43.76 ( $\Delta H$ )
		-46.82 ( $\Delta E$ ) -50.50 ( $\Delta G$ ) -52.00 ( $\Delta H$ )
		-28.70 ( $\Delta E$ ) -33.47 ( $\Delta G$ ) -28.83 ( $\Delta H$ )
		-53.76 ( $\Delta E$ ) -63.93 ( $\Delta G$ ) -50.42 ( $\Delta H$ )
		-60.50 ( $\Delta E$ ) -65.19 ( $\Delta G$ ) -63.89 ( $\Delta H$ )

### 3.4.2. Acetyl-L-Carnitine

Acetyl-L-carnitine (71) (Table 12) is an important cellular biomolecule, and carnitine esters, in general, are essential cofactors that are involved in fatty acid transport into mitochondria [87]. Once transported, the fatty acids are metabolized to supply energy for the formation of ATP. Although the linkage between an acid and carnitine is an oxygen bond, carnitine esters have large negative free energies of hydrolysis and a large group-transfer potential, which is unusual for an oxygen ester, as reported by various studies and reviews [212–216]. Computational approaches to elucidate the large group-transfer potential to the water of acetyl-L-carnitine have employed semi-empirical (AM1 [217] with the COSMO [58,218] solvent model) and quantum mechanics levels (MP2//HF/6-31G(d)) [219].

Of relevance to this article's focus on bioconjugation reactions, it has been shown that acetyl-*L*-carnitine can non-enzymatically transfer its acetyl group to proteins [34,35]. Based on this PTM and the focus of this manuscript, it was of interest to perform a detailed computational study on the relationship of the molecular structure of acetyl-*L*-carnitine to its ability to acetylate methylamine, a model for the lysine side chain. It was also hoped that this investigation might identify new carnitine analogs capable of serving as new bioconjugation reagents (Figure 4).

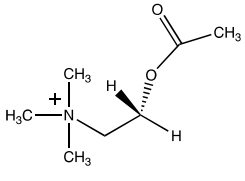
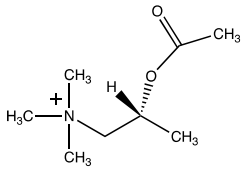
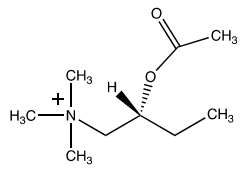
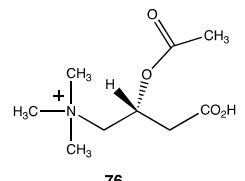
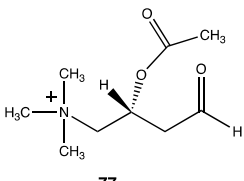
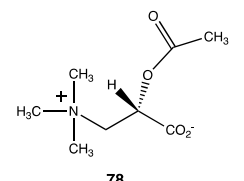
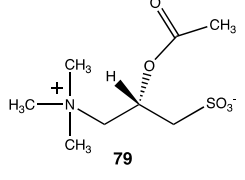
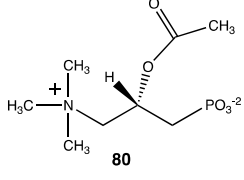
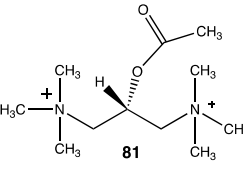
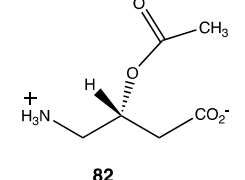
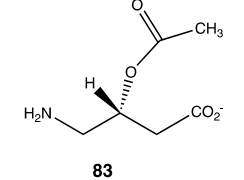
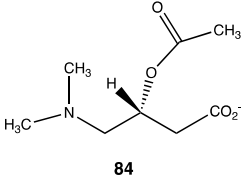
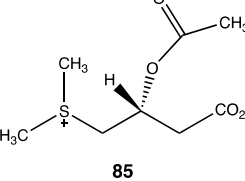
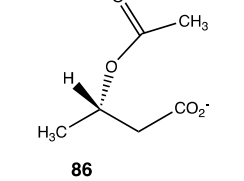
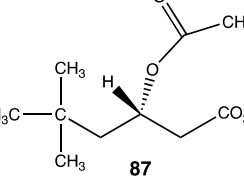
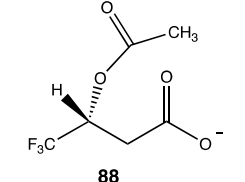
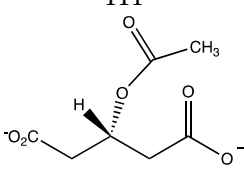
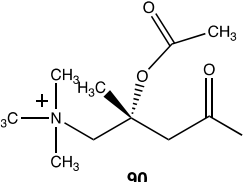
The computational investigation explored the importance of chemical structure at each of the three areas of acetyl-*L*-carnitine's molecular structure (Figure 4) to its acetyl group transfer to methylamine. In silico compounds 73–81 (Table 13) were chosen to probe the importance of the  $-\text{CH}_2-\text{CO}_2^-$  section of the molecule. The compounds were: 73 (complete removal of the  $-\text{CH}_2-\text{CO}_2^-$ ), 74 (removal of only the carboxyl group), 75 (replacing the  $\text{CO}_2^-$  with a methyl group), 76 (removal of the negative charge on the carboxyl by protonation), 77 (maintaining the oxygen functionality but replacing the carboxyl with an aldehyde moiety), 78 (removal of the intervening  $\text{CH}_2$  group from the core of the molecule), 79 and 80 (replacement of the carboxyl with a sulfonic acid or a phosphonate, respectively), and 81 (replacement of the carboxyl group with a quaternary ammonium positively charged group). For this series (Table 13), it was found by computation that a negatively charged group, such as a carboxyl (71, 78), a sulfonate (79), or a phosphonate (80) moiety, provides larger free energies of the reaction with an amine than those lacking the side chain (73) or the carboxyl but maintaining carbon atoms (74, 75), which have  $\Delta G$  values between  $-31$  and  $-37$  kJ/mol. Intermediate  $\Delta G$  values (between  $-41$  kJ/mol and  $-43$  kJ/mol) for the reaction with methylamine are found for the other modifications, such as 76, 77, and 81. It might be suggested that compounds containing the sulfonate (79) or phosphonate (80) groups might be experimentally interesting to pursue as new types of scaffolds capable of non-enzymatically transferring acyl groups to proteins.



**Figure 4.** Chemical structure of acetyl-*L*-carnitine with the three sections probed by computation. The numbers refer to the compounds in Tables 13 and 14.

Compounds 82–89 (Figure 4; Table 13) were designed to explore the quaternary ammonium section of acetyl-*L*-carnitine. Most notable in analyzing the results of these calculations is the large reduction in the favorability of the acetyl transfer if the methyl groups are removed from the amine while maintaining the positive charge, as found in compound 82, intermediate  $\Delta G$  values for compounds 83 and 84, and the large negative free energy values for the reaction when either a dimethylsulfonium (85) or a trifluoromethyl group (88) is present. Other modifications, as found in compounds 87 and 89, result in  $\Delta G$  values averaging  $-35$  kJ/mol. A comparison of the  $\Delta G$  for compound 74 ( $\Delta G = -36.86$  kJ/mol) with compound 86 ( $\Delta G = -38.20$  kJ/mol) would indicate that both areas of the acetyl-*L*-carnitine molecule are approximately equally important in providing acetyl-*L*-carnitine with its large negative  $\Delta G$  of  $-65.19$  kJ/mol for reaction with methylamine.

**Table 13.** M06-2X/cc-PVTZ(-f)++ in implicit water energies for reaction of methylamine with various acetyl-L-carnitine analogs to form N-methylacetamide.

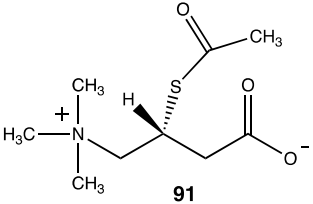
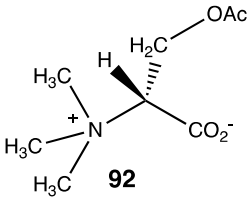
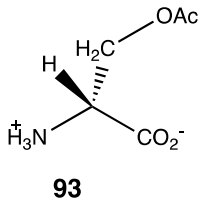
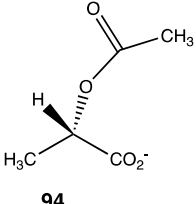
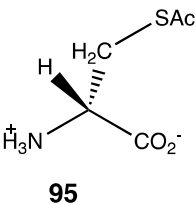
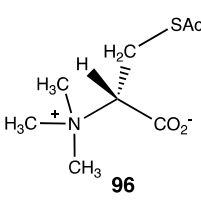
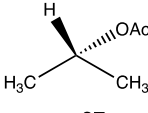
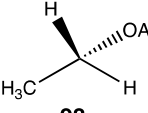
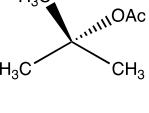
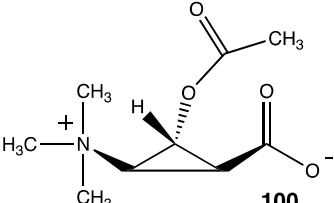
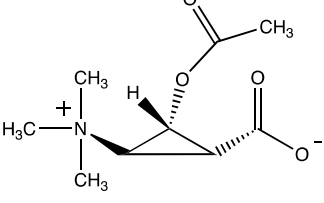
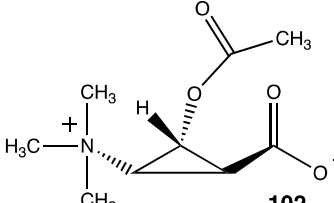
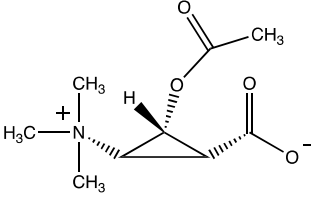
		
73	74	75
−28.83 (ΔE); −31.30 (ΔG); −31.09 (ΔH)	−33.39 (ΔE); −36.86 (ΔG); −35.73 (ΔH)	−29.41 (ΔE); −32.84 (ΔG); −31.71 (ΔH)
		
76	77	78
−40.79 (ΔE); −43.39 (ΔG); −42.84 (ΔH)	−37.95 (ΔE); −41.17 (ΔG); −40.00 (ΔH)	−43.05 (ΔE); −46.07 (ΔG); −45.56 (ΔH)
		
79	80	81
−45.65 (ΔE); −49.58 (ΔG); −45.69 (ΔH)	−72.43 (ΔE); −78.95 (ΔG); −75.19 (ΔH)	−38.07 (ΔE); −41.67 (ΔG); −39.71 (ΔH)
		
82	83	84
−21.76 (ΔE); −25.06 (ΔG); −22.59 (ΔH)	−37.91 (ΔE); −41.51 (ΔG); −41.67 (ΔH)	−40.12 (ΔE); −43.30 (ΔG); −42.97 (ΔH)
		
85	86	87
−61.59 (ΔE); −67.28 (ΔG); −62.93 (ΔH)	−36.78 (ΔE); −38.20 (ΔG); −39.66 (ΔH)	−32.51 (ΔE); −36.15 (ΔG); −33.43 (ΔH)
		
88	89	90
−52.93 (ΔE); −55.52 (ΔG); −53.26 (ΔH)	−35.27 (ΔE); −35.31 (ΔG); −37.07 (ΔH)	−71.55 (ΔE); −74.73 (ΔG); −74.73 (ΔH)

Analogs **90** (Table 13) and **91** (Table 14) explore the third section of acetyl-*L*-carnitine (Figure 4). Compound **90** replaces a hydrogen with the bulkier methyl group, resulting in a  $\Delta G = -74.73$  kJ/mol for transfer of the acetyl group to methylamine, a somewhat more favorable energetic value than acetyl-*L*-carnitine itself and likely due to the increased steric effect on the analog, which is relieved upon acetyl group transfer. Compound **91**, *S*-acetyl-*L*-thiocarnitine [220], replaces the oxygen with a sulfur atom in the ester. This thioester is somewhat less favorable than the parent compound in the acetyl transfer to methylamine ( $\Delta G = -59.75$  kJ/mol), however, it maintains most of the energetics for the acetyl transfer but does not improve upon this. This may be likely due to the longer C–S bond, which may place the acetyl group at a slightly longer distance from the carnitine scaffold and its components.

Compounds **92–99** (Table 14) are much simpler analogs of acetyl-*L*-carnitine and were designed to probe the “bare bones” of the acetyl transfer and perhaps uncover much simpler carnitine analogs to explore further as activating groups for acyl transfer to biomolecules. Compounds **92** and **93** are *L*-serine analogs, with **92** being the trimethylammonium analog of *O*-acetyl-*L*-serine and **93** being the zwitterionic form of *O*-acetyl-*L*-serine. The presence of the quaternary ammonium group in **92** appears to somewhat enhance the reaction thermodynamics compared to **93**. Replacing the protonated amine in **93** with a simple methyl group, as in compound **94**, does not alter the energetics, but replacing the oxygen in the side chain of serine with a sulfur results in *S*-acetyl-*L*-cysteine (**95**), which does dramatically alter the energetics ( $\Delta G = -60$  kJ/mol) and is comparable to acetyl-*L*-carnitine in its  $\Delta G$  value for acetyl group transfer to methylamine. It has been reported that the experimental formation of *S*-acetyl-*L*-cysteine is immediately observed to transfer the acetyl group to the  $\alpha$ -amino-forming *N*-acetyl-*L*-cysteine [221]. Hence, **95**, if formed in the cell, would likely not be able to contribute to protein modification due to this rapid internal transacylation. However, if this step is blocked by methylation of the amine, as in *N,N,N*-trimethylammonium-*L*-cysteine, **96**, the computed  $\Delta G$  was computed to be  $-55.94$  kJ/mol, which would still be favorable for protein modification. Hence, this compound could be a future source of new chemical modification reagents employing various acyl groups on the sulfur. Compounds **97–99** explore the isopropyl, ethyl, and *t*-butyl esters of acetic acid, respectively. The sterically crowded *t*-butyl ester, **99**, has the largest  $\Delta G$  of the three and is consistent with the steric crowding effect being relieved upon acetyl transfer. This would appear similar to the effect observed for compound **90**. However, based on studies on the hydrolysis of *t*-butyl esters, which invariably hydrolyze through an alkyl-oxygen unimolecular cleavage (if acid catalyzed, an  $A_{AL}1$  mechanism might be expected) [222], compounds **90** and **99** would not be useful acyl transfer reagents.

Lastly, a series of conformationally constrained analogs of acetyl-*L*-carnitine were investigated. A series of cyclopropane analogs were designed, and the thermodynamic values for their reaction with methylamine were computed (Table 14). Acetyl transfer from analogs **101** and **103** was computed to have a more favorable  $\Delta G$  of  $-55.10$  kJ/mol and  $-55.27$  kJ/mol, respectively, compared to compounds **100** and **102**, which had computed  $\Delta G$  values of  $-30.84$  kJ/mol and  $-37.45$  kJ/mol, respectively. The presence of the carboxylate group on the same side of the cyclopropane ring as the *O*-acetyl group (compounds **101**, **103**) results in more favorable  $\Delta G$  values for the acetyl transfer to methylamine, while maintaining somewhat similar  $\Delta G$  values as acetyl-*L*-carnitine itself ( $\Delta G = -65.19$  kJ/mol).

**Table 14.** M06-2X/cc-PVTZ(-f)++ in implicit water energies for reaction of methylamine with various acetyl-L-carnitine analogs to form N-methylacetamide.

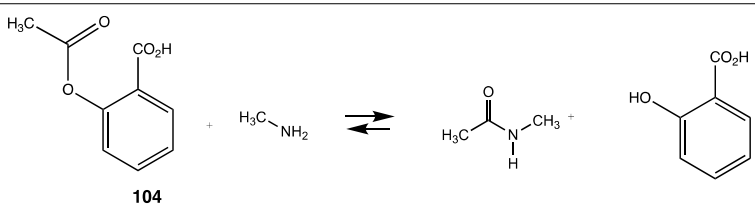
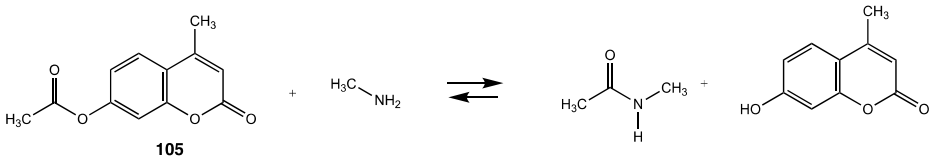
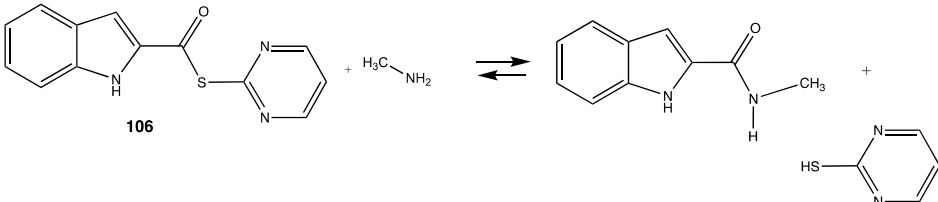
		
-59.75 ( $\Delta E$ ); -59.75 ( $\Delta G$ ); -60.71 ( $\Delta H$ )	-38.49 ( $\Delta E$ ); -42.01 ( $\Delta G$ ); -37.95 ( $\Delta H$ )	-30.67 ( $\Delta E$ ); -35.77 ( $\Delta G$ ); -30.46 ( $\Delta H$ )
		
-34.39 ( $\Delta E$ ); -37.66 ( $\Delta G$ ); -34.77 ( $\Delta H$ )	-50.96 ( $\Delta E$ ); -60.00 ( $\Delta G$ ); -54.89 ( $\Delta H$ )	-46.32 ( $\Delta E$ ); -55.94 ( $\Delta G$ ); -49.79 ( $\Delta H$ )
		
-23.43 ( $\Delta E$ ); -26.15 ( $\Delta G$ ); -23.81 ( $\Delta H$ )	-21.30 ( $\Delta E$ ); -23.35 ( $\Delta G$ ); -21.59 ( $\Delta H$ )	-36.19 ( $\Delta E$ ); -39.41 ( $\Delta G$ ); -36.57 ( $\Delta H$ )
		
-27.15 ( $\Delta E$ ); -30.84 ( $\Delta G$ ); -29.54 ( $\Delta H$ )	-52.30 ( $\Delta E$ ); -55.10 ( $\Delta G$ ); -55.27 ( $\Delta H$ )	-34.27 ( $\Delta E$ ); -37.45 ( $\Delta G$ ); -36.48 ( $\Delta H$ )
		
-53.26 ( $\Delta E$ ); -55.27 ( $\Delta G$ ); -56.23 ( $\Delta H$ )		

### 3.5. Predictive Value and Cautionary Notes

Despite the several limitations that exist for computational approaches that attempt to address complex (bio)chemical systems, the ability to employ these methods to provide insight into experimental systems is unmatched in terms of speed and predictive capability. Several insightful examples can be provided that relate to bioconjugation reactions.

Acetylsalicylic acid (ASA; aspirin), **104**, is a natural product known to have medicinal properties and whose site(s) of action have been well studied [223–226]. Calculating the thermodynamic values (Table 15) for the reaction of this molecule with methylamine provides a metric on the overall reaction-free energy for acetylation of exposed lysines on proteins. A value of  $-75.77$  kJ/mol is obtained when employing a M06-2X//cc-PVTZ (-f) ++ level of computation (C-PCM water). This value is much greater in magnitude than that of thioesters, which are known to non-enzymatically modify proteins in cells (Section 3.4.1), and the value might be used to predict that ASA should have the potential to non-enzymatically react with many proteins. It is known, of course, that ASA does acetylate enzymes such as the cyclooxygenases, its likely main target, but other proteins have also been shown to be modified by this drug [227]. In fact, a recent study employing a quantitative acid-cleavable activity-based protein profiling strategy determined at least 523 proteins in human cancer HCT116 cells are acetylated by ASA [228], and another study employing an alkyne-aspirin chemical reporter molecule detected 120 proteins that were modified in HCT-15 human cells [229]. Whether any of these acetylations add to or detract from the overall pharmacological properties of ASA is certainly an important area of research. However, the predictive capabilities of computation point to the possibility that the molecular structure of ASA has “built-in” potential for biomolecule modification and may account for its overall pharmacological profile, including its side effects and its extended uses.

**Table 15.** M06-2X/cc-PVTZ(-f)++ in implicit water energies for reaction of methylamine with various acetylsalicylic acid, acetyl coumarin, and a recently reported thioester-based antiviral agent.

Reaction	M06-2X/cc-PVTZ(-f)++ in Implicit Water (kJ/mol)
 <p style="text-align: center;"><b>104</b></p>	<p><math>-73.76</math> (<math>\Delta E</math>)</p> <p><math>-75.77</math> (<math>\Delta G</math>)</p> <p><math>-72.80</math> (<math>\Delta H</math>)</p>
 <p style="text-align: center;"><b>105</b></p>	<p><math>-60.17</math> (<math>\Delta E</math>)</p> <p><math>-63.76</math> (<math>\Delta G</math>)</p> <p><math>-59.33</math> (<math>\Delta H</math>)</p>
 <p style="text-align: center;"><b>106</b></p>	<p><math>-74.98</math> (<math>\Delta E</math>)</p> <p><math>-86.23</math> (<math>\Delta G</math>)</p> <p><math>-78.74</math> (<math>\Delta H</math>)</p>

An important area of biological and medicinal chemistry is the development of facile assays to measure enzyme activity [230,231]. These assays are frequently based on the cleavage of a substrate analog to produce an ultraviolet or fluorescent co-product capable of being readily monitored by spectrophotometric methods [232]. Two frequently employed chromophores are *p*-nitrophenol and 7-hydroxy-4-methylcoumarin. For example, esterases, proteases, and cutinases, among many hydrolytic enzymes, are monitored by the hydrolysis of *p*-nitrophenol and coumarin esters [231]. Although providing facile assay strategies, the reactivity of these types of esters can also cause protein modification-related side reactions. For example, the reaction of *p*-nitrophenyl acetate with methylamine as a model for lysine

modification was computed (Table 3) to have a  $\Delta G$  for this reaction of  $-61.89$  kJ/mol in intrinsic aqueous conditions at the M06-2X/6-311+G(2df,2p)//B3LYP/6-31G(d) level, a value indicating thermodynamic favorability. Hence, although *p*-nitrophenyl esters are routinely employed in biochemical assays, one might predict based on these DFT calculations that there is potential for chemical reaction with protein side chains by this reagent. Consistent with this prediction is the experimental report that *p*-nitrophenyl acetate itself can covalently modify the protein human serum albumin [233]. Although the rates of hydrolysis by the enzyme under study would most likely not be affected by any chemical modification, it is possible that unusual enzyme kinetics could result from time-dependent protein modification during the assay duration. It might be recommended that studies that observe unusual kinetics also include obtaining a mass spectrum of the enzyme after the kinetic assay has been completed to confirm that no labeling has occurred during the kinetic assay. Another example of a commonly employed chromophore is 7-hydroxy-4-methylcoumarin, which is frequently employed in enzyme assays such as hydrolytic enzymes. Computing the reaction thermodynamics for 7-acetoxy-4-methylcoumarin (**105**) with methylamine (Table 15) provides a  $\Delta G$  in C-PCM water of  $-63.76$  kJ/mol, a value that would indicate the possibility that this reagent could modify lysine residues on proteins. In fact, recent reports have shown that proteins can be labeled by these standard fluorescent assay substrates, confirming the predictive value of computation in this area [234–236], and further underscoring the potential for side reactions between the assay substrate and the enzyme under study.

A recent investigation has reported the development of inhibitors of SARS-CoV-2, which may provide additional therapeutic capabilities to treat this disease [237]. The molecular structure of these new compounds is based on a thioester moiety, with compound **106** (Table 15) being a reported example. These molecules were designed to inhibit the SARS-CoV-2 protease. An M06-2X//cc-PVTZ(-f) ++ level computation (C-PCM water) of its reaction with methylamine provided a value of  $-86.23$  kJ/mol for this reaction (Table 15). The magnitude of this value might alert one to the potential for these types of molecules to non-enzymatically acylate proteins, which may contribute to the overall medicinal activity of these compounds or complicate their pharmacology. Further pharmacological studies might be warranted based on this computationally based prediction.

#### 4. Conclusions

The overall reaction thermodynamics for models of a diverse set of commonly employed chemical modification reagents that react with lysine and cysteine have been computed and provide the scientific community with a basis for understanding and selecting certain chemical reagents for biochemical study. In addition, a number of cellular molecules (thioesters, acylphosphates, and acetyl-L-carnitine) were computationally studied as to their reaction with methylamine, which allows for a better understanding of the capabilities of these molecules to non-enzymatically modify proteins and is consistent with experimental results.

Lastly, two common enzyme assay substrates and two drug molecules were evaluated for their potential to modify methylamine. Calculations determined that these molecules have favorable reaction thermodynamics for acyl group transfer to lysine residues in proteins. For acetylsalicylic acid and the two common assay substrate classes, these predictions are entirely consistent with published experimental evidence. Calculation of the reaction thermodynamics for a representative of the SARS-CoV-2 protease inhibitor class recently reported predicts the potential for acyl transfer to proteins, which, if correct, may contribute to the overall pharmacology of this new class of medicinal agent. It is hoped that this study provides an additional resource for researchers involved in bioconjugation reactions and a cautionary note to those handling “routine” enzyme substrates and structurally novel medicinal agents.

**Supplementary Materials:** The following supporting information can be downloaded at: <https://www.mdpi.com/article/10.3390/compounds3030035/s1>, Table S1: T1 and G3(MP2) energies for reaction of water and methylamine with example phenyl esters; Table S2: T1 and G3(MP2) energies for reaction of water and methylamine with example phenyl esters; Table S3: T1 and G3(MP2) energies for reaction of water and methylamine with example N-hydroxysuccinimide esters; Table S4: T1 and G3(MP2) energies for reaction of water and methylamine with example carbonates; Table S5: T1 and G3(MP2) energies for reaction of water and methylamine with example isocyanates and isothiocyanates; Table S6: T1 and G3(MP2) energies for reaction of methylamine with imidates, sulfonyl chlorides, epoxides, maleimides, and 2,4-dinitrofluorobenzene; Table S7: T1 and G3(MP2) energies for reaction of methylamine with example squarate esters and aldehydes; Table S8: T1 and G3(MP2) energies for reaction of methanethiol with sulfonyl chlorides, epoxides, maleimides, and 2,4-dinitrofluorobenzene; Table S9: T1 and G3(MP2) energies for reaction of methanethiol with examples of disulfides,  $\alpha$ -bromoacids and  $\alpha$ -bromoamides, dibromomaleimides, and reaction of acetaldehyde with N-acetylhydrazide; Table S10: T1 energies for examples of common click reactions.

**Author Contributions:** Conceptualization, J.F.H.; computations, M.L., F.M. and J.F.H.; formal analysis, M.L., F.M. and J.F.H.; writing—original draft preparation, J.F.H.; writing—review and editing, M.L., F.M. and J.F.H.; supervision, J.F.H.; project administration, J.F.H.; funding acquisition, J.F.H. All authors have read and agreed to the published version of the manuscript.

**Funding:** This research was funded by NSERC (Canada) grant number RGPIN-2017-05232 (JFH), Department of Chemistry (University of Waterloo) and an NSERC CGS M (ML), and the United Arab Emirates (FM).

**Data Availability Statement:** Computational data are available by directly contacting the corresponding author.

**Acknowledgments:** Special thanks to Sean Ohlinger and Warren Hehre (Wavefunction, Inc.) for helpful advice and insightful discussions.

**Conflicts of Interest:** The authors declare no conflict of interest. The funders had no role in the design of the study; in the collection, analyses, or interpretation of data; in the writing of the manuscript; or in the decision to publish the results.

## References

1. Cserep, G.B.; Herner, A.; Kele, P. Bioorthogonal fluorescent labels: A review on combined forces. *Methods Appl. Fluoresc.* **2015**, *3*, 042001. [[CrossRef](#)]
2. Ossadnik, D.; Kuzin, S.; Qi, M.; Yulikov, M.; Godt, A. A Gd(III)-Based Spin Label at the Limits for Linewidth Reduction through Zero-Field Splitting Optimization. *Inorg. Chem.* **2023**, *62*, 408–432. [[CrossRef](#)]
3. Lundblad, R.L. *Chemical Reagents for Protein Modification*, 3rd ed.; CRC Press: Boca Raton, FL, USA, 2005.
4. Hermanson, G.T. *Bioconjugate Techniques*, 3rd ed.; Academic Press: London, UK, 2013.
5. Chen, X.; Wu, Y.W. Selective chemical labeling of proteins. *Org. Biomol. Chem.* **2016**, *14*, 5417–5439. [[CrossRef](#)]
6. Fischer, N.H.; Oliveira, M.T.; Diness, F. Chemical modification of proteins—Challenges and trends at the start of the 2020s. *Biomater. Sci.* **2023**, *11*, 719–748. [[CrossRef](#)]
7. Sornay, C.; Vaur, V.; Wagner, A.; Chaubet, G. An overview of chemo- and site-selectivity aspects in the chemical conjugation of proteins. *R. Soc. Open Sci.* **2022**, *9*, 211563. [[CrossRef](#)]
8. DeGruyter, J.N.; Malins, L.R.; Baran, P.S. Residue-Specific Peptide Modification: A Chemist's Guide. *Biochemistry* **2017**, *56*, 3863–3873. [[CrossRef](#)]
9. Reddy, N.C.; Kumar, M.; Molla, R.; Rai, V. Chemical methods for modification of proteins. *Org. Biomol. Chem.* **2020**, *18*, 4669–4691. [[CrossRef](#)]
10. Kohn, M. Immobilization strategies for small molecule, peptide and protein microarrays. *J. Pept. Sci.* **2009**, *15*, 393–397. [[CrossRef](#)]
11. Lim, C.Y.; Owens, N.A.; Wampler, R.D.; Ying, Y.; Granger, J.H.; Porter, M.D.; Takahashi, M.; Shimazu, K. Succinimidyl ester surface chemistry: Implications of the competition between aminolysis and hydrolysis on covalent protein immobilization. *Langmuir* **2014**, *30*, 12868–12878. [[CrossRef](#)]
12. O'Connell, L.; Marcoux, P.R.; Roupioz, Y. Strategies for Surface Immobilization of Whole Bacteriophages: A Review. *ACS Biomater. Sci. Eng.* **2021**, *7*, 1987–2014. [[CrossRef](#)]
13. Adumeau, P.; Sharma, S.K.; Brent, C.; Zeglis, B.M. Site-Specifically Labeled Immunoconjugates for Molecular Imaging—Part 1: Cysteine Residues and Glycans. *Mol. Imaging Biol.* **2016**, *18*, 1–17. [[CrossRef](#)] [[PubMed](#)]
14. Bai, X.; Liu, W.; Jin, S.; Zhao, W.; Xu, Y.; Zhou, Z.; Chen, S.; Pan, L. Facile Generation of Potent Bispecific Fab via Sortase A and Click Chemistry for Cancer Immunotherapy. *Cancers* **2021**, *13*, 4540. [[CrossRef](#)] [[PubMed](#)]

15. Matikonda, S.S.; McLaughlin, R.; Shrestha, P.; Lipshultz, C.; Schnermann, M.J. Structure-Activity Relationships of Antibody-Drug Conjugates: A Systematic Review of Chemistry on the Trastuzumab Scaffold. *Bioconjug. Chem.* **2022**, *33*, 1241–1253. [[CrossRef](#)] [[PubMed](#)]
16. Dozier, J.K.; Distefano, M.D. Site-Specific PEGylation of Therapeutic Proteins. *Int. J. Mol. Sci.* **2015**, *16*, 25831–25864. [[CrossRef](#)] [[PubMed](#)]
17. Vaillard, V.A.; Menegon, M.; Neuman, N.I.; Vaillard, S.E. mPEG-NHS carbonates: Effect of alkyl spacers on the reactivity: Kinetic and mechanistic insights. *J. Appl. Polym. Sci.* **2019**, *136*, 47028. [[CrossRef](#)]
18. Jayachandran, B.; Parvin, T.N.; Alam, M.M.; Chanda, K.; Mm, B. Insights on Chemical Crosslinking Strategies for Proteins. *Molecules* **2022**, *27*, 8124. [[CrossRef](#)] [[PubMed](#)]
19. Lebraud, H.; Wright, D.J.; Johnson, C.N.; Heightman, T.D. Protein Degradation by In-Cell Self-Assembly of Proteolysis Targeting Chimeras. *ACS Cent. Sci.* **2016**, *2*, 927–934. [[CrossRef](#)]
20. Reinkemeier, C.D.; Koehler, C.; Sauter, P.F.; Shymanska, N.V.; Echalié, C.; Rutkowska, A.; Will, D.W.; Schultz, C.; Lemke, E.A. Synthesis and Evaluation of Novel Ring-Strained Noncanonical Amino Acids for Residue-Specific Bioorthogonal Reactions in Living Cells. *Chemistry* **2021**, *27*, 6094–6099. [[CrossRef](#)]
21. Kim, S.; Ko, W.; Sung, B.H.; Kim, S.C.; Lee, H.S. Direct protein-protein conjugation by genetically introducing bioorthogonal functional groups into proteins. *Bioorg. Med. Chem.* **2016**, *24*, 5816–5822. [[CrossRef](#)]
22. Kuhlemann, A.; Beliu, G.; Janzen, D.; Petrini, E.M.; Taban, D.; Helmerich, D.A.; Doose, S.; Bruno, M.; Barberis, A.; Villmann, C.; et al. Genetic Code Expansion and Click-Chemistry Labeling to Visualize GABA-A Receptors by Super-Resolution Microscopy. *Front. Synaptic Neurosci.* **2021**, *13*, 727406. [[CrossRef](#)]
23. Elia, N. Using unnatural amino acids to selectively label proteins for cellular imaging: A cell biologist viewpoint. *FEBS J.* **2021**, *288*, 1107–1117. [[CrossRef](#)] [[PubMed](#)]
24. Lee, K.J.; Kang, D.; Park, H.S. Site-Specific Labeling of Proteins Using Unnatural Amino Acids. *Mol. Cells* **2019**, *42*, 386–396. [[CrossRef](#)] [[PubMed](#)]
25. Urquhart, T.; Daub, E.; Honek, J.F. Bioorthogonal Modification of the Major Sheath Protein of Bacteriophage M13: Extending the Versatility of Bionanomaterial Scaffolds. *Bioconjug. Chem.* **2016**, *27*, 2276–2280. [[CrossRef](#)] [[PubMed](#)]
26. Urquhart, T.; Howie, B.; Zhang, L.; Leung, K.T.; Honek, J.F. Bioconjugation of Bacteriophage Pf1 and Extension to Pf1-Based Bionanomaterials. *Curr. Nanosci.* **2021**, *17*, 139–150. [[CrossRef](#)]
27. Battigelli, A.; Almeida, B.; Shukla, A. Recent Advances in Bioorthogonal Click Chemistry for Biomedical Applications. *Bioconjug. Chem.* **2022**, *33*, 263–271. [[CrossRef](#)]
28. Taiariol, L.; Chaix, C.; Farre, C.; Moreau, E. Click and Bioorthogonal Chemistry: The Future of Active Targeting of Nanoparticles for Nanomedicines? *Chem. Rev.* **2022**, *122*, 340–384. [[CrossRef](#)]
29. Stump, B. Click Bioconjugation: Modifying Proteins Using Click-Like Chemistry. *Chembiochem* **2022**, *23*, e202200016. [[CrossRef](#)]
30. Moreno-Yruela, C.; Baek, M.; Monda, F.; Olsen, C.A. Chiral Posttranslational Modification to Lysine epsilon-Amino Groups. *Acc. Chem. Res.* **2022**, *55*, 1456–1466. [[CrossRef](#)]
31. Christensen, D.G.; Xie, X.; Basisty, N.; Byrnes, J.; McSweeney, S.; Schilling, B.; Wolfe, A.J. Post-translational Protein Acetylation: An Elegant Mechanism for Bacteria to Dynamically Regulate Metabolic Functions. *Front. Microbiol.* **2019**, *10*, 1604. [[CrossRef](#)]
32. Trub, A.G.; Hirschev, M.D. Reactive Acyl-CoA Species Modify Proteins and Induce Carbon Stress. *Trends Biochem. Sci.* **2018**, *43*, 369–379. [[CrossRef](#)]
33. Kuhn, M.L.; Zemaitaitis, B.; Hu, L.I.; Sahu, A.; Sorensen, D.; Minasov, G.; Lima, B.P.; Scholle, M.; Mrksich, M.; Anderson, W.F.; et al. Structural, kinetic and proteomic characterization of acetyl phosphate-dependent bacterial protein acetylation. *PLoS ONE* **2014**, *9*, e94816. [[CrossRef](#)]
34. Pettegrew, J.W.; Levine, J.; McClure, R.J. Acetyl-L-carnitine physical-chemical, metabolic, and therapeutic properties: Relevance for its mode of action in Alzheimer's disease and geriatric depression. *Mol. Psychiatry* **2000**, *5*, 616–632. [[CrossRef](#)]
35. Swamy-Mruthinti, S.; Carter, A.L. Acetyl-L-carnitine decreases glycation of lens proteins: In vitro studies. *Exp. Eye Res.* **1999**, *69*, 109–115. [[CrossRef](#)] [[PubMed](#)]
36. Shao, Y.; Molnar, L.F.; Jung, Y.; Kussmann, J.; Ochsenfeld, C.; Brown, S.T.; Gilbert, A.T.; Slipchenko, L.V.; Levchenko, S.V.; O'Neill, D.P.; et al. Advances in methods and algorithms in a modern quantum chemistry program package. *Phys. Chem. Chem. Phys.* **2006**, *8*, 3172–3191. [[CrossRef](#)]
37. Tirado-Rives, J.; Jorgensen, W.L. Performance of B3LYP density functional methods for a large set of organic molecules. *J. Chem. Theory Comput.* **2008**, *4*, 297–306. [[CrossRef](#)]
38. Lu, L.L. Can B3LYP be Improved by Optimization of the Proportions of Exchange and Correlation Functionals? *Int. J. Quantum Chem.* **2015**, *115*, 502–509. [[CrossRef](#)]
39. Zhao, Y.; Truhlar, D.G. The M06 suite of density functionals for main group thermochemistry, thermochemical kinetics, noncovalent interactions, excited states, and transition elements: Two new functionals and systematic testing of four M06-class functionals and 12 other functionals. *Theor. Chem. Acc.* **2008**, *120*, 215–241. [[CrossRef](#)]
40. Goerigk, L.; Hansen, A.; Bauer, C.; Ehrlich, S.; Najibi, A.; Grimme, S. A look at the density functional theory zoo with the advanced GMTKN55 database for general main group thermochemistry, kinetics and noncovalent interactions. *Phys. Chem. Chem. Phys.* **2017**, *19*, 32184–32215. [[CrossRef](#)]

41. Ohlinger, W.S.; Klunzinger, P.E.; Deppmeier, B.J.; Hehre, W.J. Efficient Calculation of Heats of Formation. *J. Phys. Chem. A* **2009**, *113*, 2165–2175. [[CrossRef](#)] [[PubMed](#)]
42. Curtiss, L.A.; Redfern, P.C.; Raghavachari, K.; Rassolov, V.; Pople, J.A. Gaussian-3 theory using reduced Moller-Plesset order. *J. Chem. Phys.* **1999**, *110*, 4703–4709. [[CrossRef](#)]
43. Halgren, T.A. Merck molecular force field. 5. Extension of MMFF94 using experimental data, additional computational data, and empirical rules. *J. Comput. Chem.* **1996**, *17*, 616–641. [[CrossRef](#)]
44. Halgren, T.A. Merck molecular force field. 1. Basis, form, scope, parameterization, and performance of MMFF94. *J. Comput. Chem.* **1996**, *17*, 490–519. [[CrossRef](#)]
45. NIST. *NIST Computational Chemistry Comparison and Benchmark Database*; Johnson, R.D., III, Ed.; NIST: Gaithersburg, MD, USA, 2022.
46. Hehre, W.J. *A Guide to Molecular Mechanics and Quantum Chemical Calculations*; Wavefunction, Inc.: Irvine, CA, USA, 2003.
47. Costa, A.M.; Bosch, L.; Petit, E.; Vilarrasa, J. Computational Study of the Addition of Methanethiol to 40+ Michael Acceptors as a Model for the Bioconjugation of Cysteines. *J. Org. Chem.* **2021**, *86*, 7107–7118. [[CrossRef](#)] [[PubMed](#)]
48. Wavefunction, I. *Spartan'20: Tutorial and User's Guide*; Wavefunction, Inc.: Irvine, CA, USA, 2022.
49. Cossi, M.; Rega, N.; Scalmani, G.; Barone, V. Energies, structures, and electronic properties of molecules in solution with the C-PCM solvation model. *J. Comput. Chem.* **2003**, *24*, 669–681. [[CrossRef](#)]
50. Skyner, R.E.; McDonagh, J.L.; Groom, C.R.; van Mourik, T.; Mitchell, J.B.O. A review of methods for the calculation of solution free energies and the modelling of systems in solution. *Phys. Chem. Chem. Phys.* **2015**, *17*, 6174–6191. [[CrossRef](#)]
51. Bochevarov, A.D.; Harder, E.; Hughes, T.F.; Greenwood, J.R.; Braden, D.A.; Philipp, D.M.; Rinaldo, D.; Halls, M.D.; Zhang, J.; Friesner, R.A. Jaguar: A high-performance quantum chemistry software program with strengths in life and materials sciences. *Int. J. Quantum Chem.* **2013**, *113*, 2110–2142. [[CrossRef](#)]
52. Cao, Y.; Halls, M.D.; Vadicherla, T.R.; Friesner, R.A. Pseudospectral implementations of long-range corrected density functional theory. *J. Comput. Chem.* **2021**, *42*, 2089–2102. [[CrossRef](#)]
53. Harder, E.; Damm, W.; Maple, J.; Wu, C.; Reboul, M.; Xiang, J.Y.; Wang, L.; Lupyan, D.; Dahlgren, M.K.; Knight, J.L.; et al. OPLS3: A Force Field Providing Broad Coverage of Drug-like Small Molecules and Proteins. *J. Chem. Theory Comput.* **2016**, *12*, 281–296. [[CrossRef](#)] [[PubMed](#)]
54. Lu, C.; Wu, C.; Ghoreishi, D.; Chen, W.; Wang, L.; Damm, W.; Ross, G.A.; Dahlgren, M.K.; Russell, E.; Von Bargen, C.D.; et al. OPLS4: Improving Force Field Accuracy on Challenging Regimes of Chemical Space. *J. Chem. Theory Comput.* **2021**, *17*, 4291–4300. [[CrossRef](#)]
55. Parish, C.A.; Still, W.C. MacroModel. The computational chemists molecular modeling tool. *Abstr. Pap. Am. Chem. S* **1996**, *211*, 90-Comp.
56. Stewart, J.J.P. Optimization of Parameters for Semiempirical Methods. 1. Method. *J. Comput. Chem.* **1989**, *10*, 209–220. [[CrossRef](#)]
57. Stewart, J.J.P. Optimization of Parameters for Semiempirical Methods. 2. Applications. *J. Comput. Chem.* **1989**, *10*, 221–264. [[CrossRef](#)]
58. Klamt, A.; Schuurmann, G. COSMO: A New Approach to Dielectric Screening in Solvents with Explicit Expressions for the Screening Energy and Its Gradient. *J. Chem. Soc. Perkin Trans. 2* **1993**, *5*, 799–805. [[CrossRef](#)]
59. Bondi, A. Van Der Waals Volumes + Radii. *J. Phys. Chem* **1964**, *68*, 441–451. [[CrossRef](#)]
60. Moellering, R.E.; Cravatt, B.F. Functional lysine modification by an intrinsically reactive primary glycolytic metabolite. *Science* **2013**, *341*, 549–553. [[CrossRef](#)] [[PubMed](#)]
61. James, A.M.; Smith, C.L.; Smith, A.C.; Robinson, A.J.; Hoogewijs, K.; Murphy, M.P. The Causes and Consequences of Nonenzymatic Protein Acylation. *Trends Biochem. Sci.* **2018**, *43*, 921–932. [[CrossRef](#)]
62. Fraenkel-Conrat, H. Methods for investigating the essential groups for enzyme activity. In *Meth Enzymol*; Colowick, S.P., Kaplan, N.O., Eds.; Academic Press: New York, NY, USA, 1959; Volume 4, pp. 247–269.
63. Smyth, D.G. Acetylation of amino and tyrosine hydroxyl groups. Preparation of inhibitors of oxytocin with no intrinsic activity on the isolated uterus. *J. Biol. Chem.* **1967**, *242*, 1592–1598. [[CrossRef](#)] [[PubMed](#)]
64. Spanedda, M.V.; Bourel-Bonnet, L. Cyclic Anhydrides as Powerful Tools for Bioconjugation and Smart Delivery. *Bioconjug. Chem.* **2021**, *32*, 482–496. [[CrossRef](#)]
65. Hori, K. Theoretical study of a reaction path via a hydrogen-bonded intermediate for the alkaline hydrolysis of esters in the gas phase. *J. Chem. Soc. Perkin Trans. 2* **1992**, *1992*, 1629–1633. [[CrossRef](#)]
66. Zhan, C.-G.; Landry, D.W.; Ornstein, R.L. Theoretical Studies of Fundamental Pathways for Alkaline Hydrolysis of Carboxylic Acid Esters in Gas Phase. *J. Am. Chem. Soc.* **2000**, *122*, 1522–1530. [[CrossRef](#)]
67. Zhan, C.-G.; Landry, D.W.; Ornstein, R.L. Reaction Pathways and Energy Barriers for Alkaline Hydrolysis of Carboxylic Acid Esters in Water Studied by a Hybrid Supermolecule-Polarizable Continuum Approach. *J. Am. Chem. Soc.* **2000**, *122*, 2621–2627. [[CrossRef](#)]
68. Hori, K.; Ikenaga, Y.; Arata, K.; Takahashi, T.; Kasai, K.; Noguchi, Y.; Sumimoto, M.; Yamamoto, H. Theoretical study on the reaction mechanism for the hydrolysis of esters and amides under acidic conditions. *Tetrahedron* **2007**, *63*, 1264–1269. [[CrossRef](#)]
69. Martin, R.B. Mechanisms of Acid Hydrolysis of Carboxylic Acid Esters and Amides. *J. Am. Chem. Soc.* **1962**, *84*, 4130–4136. [[CrossRef](#)]

70. Limpanuparb, T.; Punyain, K.; Tantirungrotechai, Y. A DFT investigation of methanolysis and hydrolysis of triacetin. *J. Mol. Struct. THEOCHEM* **2010**, *955*, 23–32. [[CrossRef](#)]
71. Kallies, B.; Mitzner, R. Models of water-assisted hydrolyses of methyl formate, formamide, and urea from combined DFT-SCRF calculations. *J. Mol. Model.* **1998**, *4*, 183–196. [[CrossRef](#)]
72. Allen, S.E.; Hsieh, S.Y.; Gutierrez, O.; Bode, J.W.; Kozlowski, M.C. Concerted Amidation of Activated Esters: Reaction Path and Origins of Selectivity in the Kinetic Resolution of Cyclic Amines via N-Heterocyclic Carbenes and Hydroxamic Acid Cocatalyzed Acyl Transfer. *J. Am. Chem. Soc.* **2014**, *136*, 11783–11791. [[CrossRef](#)] [[PubMed](#)]
73. Shi, H.; Wang, Y.; Hua, R. Acid-catalyzed carboxylic acid esterification and ester hydrolysis mechanism: Acylium ion as a sharing active intermediate via a spontaneous trimolecular reaction based on density functional theory calculation and supported by electrospray ionization-mass spectrometry. *Phys. Chem. Chem. Phys.* **2015**, *17*, 30279–30291. [[CrossRef](#)] [[PubMed](#)]
74. Fox, J.M.; Dmitrenko, O.; Liao, L.A.; Bach, R.D. Computational studies of nucleophilic substitution at carbonyl carbon: The S(N)2 mechanism versus the tetrahedral intermediate in organic synthesis. *J. Org. Chem.* **2004**, *69*, 7317–7328. [[CrossRef](#)]
75. Yang, W.; Drueckhammer, D.G. Computational studies of the aminolysis of oxoesters and thioesters in aqueous solution. *Org. Lett.* **2000**, *2*, 4133–4136. [[CrossRef](#)]
76. Yang, W.; Drueckhammer, D.G. Understanding the relative acyl-transfer reactivity of oxoesters and thioesters: Computational analysis of transition state delocalization effects. *J. Am. Chem. Soc.* **2001**, *123*, 11004–11009. [[CrossRef](#)] [[PubMed](#)]
77. Wang, L.H.; Zipse, H. Bifunctional catalysis of ester aminolysis—A computational and experimental study. *Liebigs. Ann. Recl.* **1996**, *1996*, 1501–1509. [[CrossRef](#)]
78. Galabov, B.; Atanasov, Y.; Ilieva, S.; Schaefer, H.F. Mechanism of the Aminolysis of Methyl Benzoate: A Computational Study. *J. Phys. Chem. A* **2005**, *109*, 11470–11474. [[CrossRef](#)] [[PubMed](#)]
79. Ikhazuangbe, P.M.O.; Adama, K.K. Experimental Investigation of the Kinetics and Thermodynamics of the Production of Methanol from the Hydrolysis of Methyl Acetate Catalyzed with Hydrochloric Acid. *Int. J. Chem. Chem. Process.* **2021**, *7*, 13–25.
80. Shi, Z.; Hsieh, Y.H.; Weinberg, N.; Wolfe, S. The neutral hydrolysis of methyl acetate—Part 2. Is there a tetrahedral intermediate? *Can. J. Chem.* **2009**, *87*, 544–555. [[CrossRef](#)]
81. Kruger, H.G. Ab initio mechanistic study of the protection of alcohols and amines with anhydrides. *J. Mol. Struct. THEOCHEM* **2002**, *577*, 281–285. [[CrossRef](#)]
82. Petrova, T.; Okovytyy, S.; Gorb, L.; Leszczynski, J. Computational study of the aminolysis of anhydrides: Effect of the catalysis to the reaction of succinic anhydride with methylamine in gas phase and nonpolar solution. *J. Phys. Chem. A* **2008**, *112*, 5224–5235. [[CrossRef](#)]
83. Ruff, F.; Farkas, O. Concerted S(N)2 mechanism for the hydrolysis of acid chlorides: Comparisons of reactivities calculated by the density functional theory with experimental data. *J. Phys. Org. Chem.* **2011**, *24*, 480–491. [[CrossRef](#)]
84. Vlasov, V.M. Substituent effects in substrates on activation parameters in the bimolecular nucleophilic reactions in solution. *New J. Chem.* **2010**, *34*, 2962–2970. [[CrossRef](#)]
85. Chandru, K.; Gilbert, A.; Butch, C.; Aono, M.; Cleaves, H.J. The Abiotic Chemistry of Thiolated Acetate Derivatives and the Origin of Life. *Sci. Rep.* **2016**, *6*, 29883. [[CrossRef](#)] [[PubMed](#)]
86. Agouridas, V.; El Mahdi, O.; Diemer, V.; Cargoet, M.; Monbaliu, J.M.; Melnyk, O. Native Chemical Ligation and Extended Methods: Mechanisms, Catalysis, Scope, and Limitations. *Chem. Rev.* **2019**, *119*, 7328–7443. [[CrossRef](#)]
87. Voet, D.; Voet, J.G.; Pratt, C.W. *Fundamentals of Biochemistry*, 5th ed.; John Wiley & Sons: Hoboken, NJ, USA, 2016.
88. Kulkarni, R.A.; Worth, A.J.; Zengeya, T.T.; Shrimp, J.H.; Garlick, J.M.; Roberts, A.M.; Montgomery, D.C.; Sourbier, C.; Gibbs, B.K.; Mesaros, C.; et al. Discovering Targets of Non-enzymatic Acylation by Thioester Reactivity Profiling. *Cell Chem. Biol.* **2017**, *24*, 231–242. [[CrossRef](#)]
89. Wagner, G.R.; Bhatt, D.P.; O’Connell, T.M.; Thompson, J.W.; Dubois, L.G.; Backos, D.S.; Yang, H.; Mitchell, G.A.; Ilkayeva, O.R.; Stevens, R.D.; et al. A Class of Reactive Acyl-CoA Species Reveals the Non-enzymatic Origins of Protein Acylation. *Cell Metab.* **2017**, *25*, 823–837.e8. [[CrossRef](#)]
90. Guthrie, J.P. Hydration of Thioesters—Evaluation of Free-Energy Changes for Addition of Water to Some Thioesters, Rate-Equilibrium Correlations over Very Wide Ranges in Equilibrium-Constants, and a New Mechanistic Criterion. *J. Am. Chem. Soc.* **1978**, *100*, 5892–5904. [[CrossRef](#)]
91. Jencks, W.P.; Gilchrist, M. Free Energies of Hydrolysis of Some Esters + Thiol Esters of Acetic Acid. *J. Am. Chem. Soc.* **1964**, *86*, 4651–4654. [[CrossRef](#)]
92. Slosarczyk, A.T.; Ramapanicker, R.; Norberg, T.; Baltzer, L. Mixed pentafluorophenyl and o-fluorophenyl esters of aliphatic dicarboxylic acids: Efficient tools for peptide and protein conjugation. *RSC Adv.* **2012**, *2*, 908–914. [[CrossRef](#)]
93. Wang, J.; Zhang, R.Y.; Wang, Y.C.; Chen, X.Z.; Yin, X.G.; Du, J.J.; Lei, Z.; Xin, L.M.; Gao, X.F.; Liu, Z.; et al. Polyfluorophenyl Ester-Terminated Homobifunctional Cross-Linkers for Protein Conjugation. *Synlett* **2017**, *28*, 1934–1938. [[CrossRef](#)]
94. Lomant, A.J.; Fairbanks, G. Chemical probes of extended biological structures: Synthesis and properties of the cleavable protein cross-linking reagent [<sup>35</sup>S]dithiobis(succinimidyl propionate). *J. Mol. Biol.* **1976**, *104*, 243–261. [[CrossRef](#)] [[PubMed](#)]
95. Cuatrecasas, P.; Parikh, I. Adsorbents for affinity chromatography. Use of N-hydroxysuccinimide esters of agarose. *Biochemistry* **1972**, *11*, 2291–2299. [[CrossRef](#)]
96. Rao, H.B.; Wang, Y.Y.; Zeng, X.Y.; Xue, Y.; Li, Z.R. Theoretical study on the aminolysis of p-substituted phenyl acetates with dimeric ammonia in vacuo and acetonitrile. *Comput. Theor. Chem.* **2013**, *1008*, 8–14. [[CrossRef](#)]

97. Sung, D.D.; Koo, I.S.; Yang, K.; Lee, I. DFT studies on the structure and stability of zwitterionic tetrahedral intermediate in the aminolysis of esters. *Chem. Phys. Lett.* **2006**, *426*, 280–284. [[CrossRef](#)]
98. Yi, G.Q.; Zeng, Y.; Xia, X.F.; Xue, Y.; Kim, C.K.; Yan, G.S. The substituent effects of the leaving groups on the aminolysis of phenyl acetates: DFT studies. *Chem. Phys.* **2008**, *345*, 73–81. [[CrossRef](#)]
99. Andres, G.O.; Pierini, A.B.; de Rossi, R.H. Kinetic and theoretical studies on the mechanism of intramolecular catalysis in phenyl ester hydrolysis. *J. Org. Chem.* **2006**, *71*, 7650–7656. [[CrossRef](#)] [[PubMed](#)]
100. Xia, S.; Zhang, H. Density functional theory study of selective deacylation of aromatic acetate in the presence of aliphatic acetate under ammonium acetate mediated conditions. *J. Org. Chem.* **2014**, *79*, 6135–6142. [[CrossRef](#)]
101. Xie, D.; Zhou, Y.; Xu, D.; Guo, H. Solvent effect on concertedness of the transition state in the hydrolysis of p-nitrophenyl acetate. *Org. Lett.* **2005**, *7*, 2093–2095. [[CrossRef](#)] [[PubMed](#)]
102. Elzahhar, P.; Belal, A.S.F.; Elamrawy, F.; Helal, N.A.; Nounou, M.I. Bioconjugation in Drug Delivery: Practical Perspectives and Future Perceptions. *Methods Mol. Biol.* **2019**, *2000*, 125–182. [[CrossRef](#)] [[PubMed](#)]
103. Dempsey, D.R.; Jiang, H.; Kalin, J.H.; Chen, Z.; Cole, P.A. Site-Specific Protein Labeling with N-Hydroxysuccinimide-Esters and the Analysis of Ubiquitin Ligase Mechanisms. *J. Am. Chem. Soc.* **2018**, *140*, 9374–9378. [[CrossRef](#)]
104. Staros, J.V. N-hydroxysulfosuccinimide active esters: Bis(N-hydroxysulfosuccinimide) esters of two dicarboxylic acids are hydrophilic, membrane-impermeant, protein cross-linkers. *Biochemistry* **1982**, *21*, 3950–3955. [[CrossRef](#)]
105. Bu, J.; Fisher, C.M.; Gilbert, J.D.; Prentice, B.M.; McLuckey, S.A. Selective Covalent Chemistry via Gas-Phase Ion/ion Reactions: An Exploration of the Energy Surfaces Associated with N-Hydroxysuccinimide Ester Reagents and Primary Amines and Guanidine Groups. *J. Am. Soc. Mass. Spectrom.* **2016**, *27*, 1089–1098. [[CrossRef](#)]
106. Morpurgo, M.; Bayer, E.A.; Wilchek, M. N-hydroxysuccinimide carbonates and carbamates are useful reactive reagents for coupling ligands to lysines on proteins. *J. Biochem. Biophys. Methods* **1999**, *38*, 17–28. [[CrossRef](#)]
107. Zalipsky, S.; Seltzer, R.; Menon-Rudolph, S. Evaluation of a new reagent for covalent attachment of polyethylene glycol to proteins. *Biotechnol. Appl. Biochem.* **1992**, *15*, 100–114. [[CrossRef](#)]
108. Hu, H.; Luo, C.; Wang, B.; Lai, T.; Zhang, G.; Gao, G. NaCl catalyzed transesterification and hydrolysis of ethylene carbonate. *Mol. Catal.* **2023**, *538*, 113010. [[CrossRef](#)]
109. Chen, R.; Luo, X.L.; Liang, G.M. Theoretical studies on the aminolysis mechanism of propylene carbonate with ammonia. *Theor. Chem. Acc.* **2015**, *134*, 32. [[CrossRef](#)]
110. Zabalov, M.V.; Tiger, R.P.; Berlin, A.A. Mechanism of urethane formation from cyclocarbonates and amines: A quantum chemical study. *Russ. Chem. B* **2012**, *61*, 518–527. [[CrossRef](#)]
111. Zabalov, M.V.; Levina, M.A.; Tiger, R.P. Molecular Organization of Reagents in the Kinetics and Catalysis of Liquid-Phase Reactions: XIII. Cyclic Transition States Involving Solvent Molecules in the Mechanism of Aminolysis of Cyclocarbonates in an Alcohol Medium. *Kinet. Catal.* **2020**, *61*, 721–729. [[CrossRef](#)]
112. Karlsson, I.; Samuelsson, K.; Ponting, D.J.; Tornqvist, M.; Ilag, L.L.; Nilsson, U. Peptide Reactivity of Isothiocyanates—Implications for Skin Allergy. *Sci. Rep.* **2016**, *6*, 21203. [[CrossRef](#)]
113. Topuz, F.; Bartneck, M.; Pan, Y.; Tacke, F. One-Step Fabrication of Biocompatible Multifaceted Nanocomposite Gels and Nanolayers. *Biomacromolecules* **2017**, *18*, 386–397. [[CrossRef](#)]
114. Wang, K.; Wang, D.; Ji, K.; Chen, W.; Zheng, Y.; Dai, C.; Wang, B. Post-synthesis DNA modifications using a trans-cyclooctene click handle. *Org. Biomol. Chem.* **2015**, *13*, 909–915. [[CrossRef](#)]
115. Longo, B.; Zanato, C.; Piras, M.; Dall'Angelo, S.; Windhorst, A.D.; Vugts, D.J.; Baldassarre, M.; Zanda, M. Design, Synthesis, Conjugation, and Reactivity of Novel trans,trans-1,5-Cyclooctadiene-Derived Bioorthogonal Linkers. *Bioconjug. Chem.* **2020**, *31*, 2201–2210. [[CrossRef](#)]
116. Yuan, Y.; Cao, J.P.; Liu, Y.L.; Shi, A.J.; Zhang, Q.; Lin, X.X.; Wang, M.L. Catalytic Effects of Water Clusters on the Hydrolysis of Toluene-2,4-diisocyanate: A DFT Study. *B Chem. Soc. Jpn.* **2016**, *89*, 74–91. [[CrossRef](#)]
117. Davies, G.E.; Stark, G.R. Use of dimethyl suberimidate, a cross-linking reagent, in studying the subunit structure of oligomeric proteins. *Proc. Natl. Acad. Sci. USA* **1970**, *66*, 651–656. [[CrossRef](#)]
118. Uchiumi, T.; Terao, K.; Ogata, K. Identification of neighboring protein pairs in rat liver 60S ribosomal subunits cross-linked with dimethyl suberimidate or dimethyl 3,3'-dithiobispropionimidate. *J. Biochem.* **1980**, *88*, 1033–1044. [[CrossRef](#)] [[PubMed](#)]
119. Seong, H.; Park, J.; Bae, M.; Shin, S. Rapid and Efficient Extraction of Cell-Free DNA Using Homobifunctional Crosslinkers. *Biomedicines* **2022**, *10*, 1883. [[CrossRef](#)]
120. Begum, M.F.; Varghese, H.T.; Mary, Y.S.; Panicker, C.Y.; Salim, M.A. Structural defects in imidates: An ab initio Study. *Int. J. Chem. Sci.* **2011**, *9*, 1763–1767.
121. Mossberg, K.; Ericsson, M. Detection of doubly stained fluorescent specimens using confocal microscopy. *J. Microsc.* **1990**, *158*, 215–224. [[CrossRef](#)] [[PubMed](#)]
122. Yamabe, S.; Zeng, G.X.; Guan, W.; Sakaki, S. SN1-SN2 and SN2-SN3 Mechanistic Changes Revealed by Transition States of the Hydrolyses of Benzyl Chlorides and Benzenesulfonyl Chlorides. *J. Comput. Chem.* **2014**, *35*, 1140–1148. [[CrossRef](#)]
123. Ivanov, S.N.; Kislov, V.V.; Gnedin, B.G. Solvation effects in hydrolysis of 2-toluenesulfonyl halides in aqueous dioxane. Catalysis with water molecules in cyclic transition states. *Russ. J. Gen. Chem.* **2004**, *74*, 95–100. [[CrossRef](#)]

124. Ivanov, S.N.; Kislov, V.V.; Gnedin, B.G. Simulation of benzenesulfonyl chloride hydrolysis. Influence of the size and structural ordering of aqueous clusters on thermodynamic and activation parameters of the process. *Russ. J. Gen. Chem.* **2004**, *74*, 86–94. [[CrossRef](#)]
125. Rodrigues, R.C.; Berenguer-Murcia, A.; Carballares, D.; Morellon-Sterling, R.; Fernandez-Lafuente, R. Stabilization of enzymes via immobilization: Multipoint covalent attachment and other stabilization strategies. *Biotechnol. Adv.* **2021**, *52*, 107821. [[CrossRef](#)]
126. Lundin, A.; Panas, I.; Ahlberg, E. A mechanistic investigation of ethylene oxide hydrolysis to ethanediol. *J. Phys. Chem. A* **2007**, *111*, 9087–9092. [[CrossRef](#)]
127. Muniz Filho, R.C.D.; Sousa, S.A.A.d.; Pereira, F.d.S.; Ferreira, M.M.C. Theoretical Study of Acid-Catalyzed Hydrolysis of Epoxides. *J. Phys. Chem. A* **2010**, *114*, 5187–5194. [[CrossRef](#)]
128. Piletic, I.R.; Edney, E.O.; Bartolotti, L.J. A computational study of acid catalyzed aerosol reactions of atmospherically relevant epoxides. *Phys. Chem. Chem. Phys.* **2013**, *15*, 18065–18076. [[CrossRef](#)]
129. Renault, K.; Fredy, J.W.; Renard, P.Y.; Sabot, C. Covalent Modification of Biomolecules through Maleimide-Based Labeling Strategies. *Bioconjug. Chem.* **2018**, *29*, 2497–2513. [[CrossRef](#)] [[PubMed](#)]
130. Ravasco, J.; Faustino, H.; Trindade, A.; Gois, P.M.P. Bioconjugation with Maleimides: A Useful Tool for Chemical Biology. *Chemistry* **2019**, *25*, 43–59. [[CrossRef](#)] [[PubMed](#)]
131. Wong, S.S.; Jameson, D.M. *Chemistry of Protein and Nucleic Acid Cross-Linking and Conjugation*, 2nd ed.; CRC Press: Boca Raton, FL, USA, 2012.
132. Nakane, P.K. Recent progress in the peroxidase-labeled antibody method. *Ann. N. Y. Acad. Sci.* **1975**, *254*, 203–211. [[CrossRef](#)] [[PubMed](#)]
133. Jose, K.B.; Cyriac, J.; Moolayil, J.T.; Sebastian, V.S.; George, M. The mechanism of aromatic nucleophilic substitution reaction between ethanolamine and fluoro-nitrobenzenes: An investigation by kinetic measurements and DFT calculations. *J. Phys. Org. Chem.* **2011**, *24*, 714–719. [[CrossRef](#)]
134. Cramer, C.J.; Truhlar, D.G. A Universal Approach to Solvation Modeling. *Acc. Chem. Res.* **2008**, *41*, 760–768. [[CrossRef](#)] [[PubMed](#)]
135. Ratto, A.; Honek, J.F. Oxocarbon Acids and their Derivatives in Biological and Medicinal Chemistry. *Curr. Med. Chem.* **2023**. [[CrossRef](#)]
136. Storer, R.I.; Aciro, C.; Jones, L.H. Squaramides: Physical properties, synthesis and applications. *Chem. Soc. Rev.* **2011**, *40*, 2330–2346. [[CrossRef](#)]
137. Chasak, J.; Slachtova, V.; Urban, M.; Brulikova, L. Squaric acid analogues in medicinal chemistry. *Eur. J. Med. Chem.* **2021**, *209*, 112872. [[CrossRef](#)]
138. Agnew-Francis, K.A.; Williams, C.M. Squaramides as Bioisosteres in Contemporary Drug Design. *Chem. Rev.* **2020**, *120*, 11616–11650. [[CrossRef](#)]
139. Dingels, C.; Wurm, F.; Wagner, M.; Klok, H.A.; Frey, H. Squaric acid mediated chemoselective PEGylation of proteins: Reactivity of single-step-activated alpha-amino poly(ethylene glycol)s. *Chemistry* **2012**, *18*, 16828–16835. [[CrossRef](#)] [[PubMed](#)]
140. Wurm, F.R.; Klok, H.A. Be squared: Expanding the horizon of squaric acid-mediated conjugations. *Chem. Soc. Rev.* **2013**, *42*, 8220–8236. [[CrossRef](#)] [[PubMed](#)]
141. Xu, P.; Kelly, M.; Vann, W.F.; Qadri, F.; Ryan, E.T.; Kovac, P. Conjugate Vaccines from Bacterial Antigens by Squaric Acid Chemistry: A Closer Look. *Chembiochem* **2017**, *18*, 799–815. [[CrossRef](#)] [[PubMed](#)]
142. Xu, P.; Trinh, M.N.; Kovac, P. Conjugation of carbohydrates to proteins using di(triethylene glycol monomethyl ether) squaric acid ester revisited. *Carbohydr. Res.* **2018**, *456*, 24–29. [[CrossRef](#)]
143. Suleymanoglu, N.; Ustabas, R.; Alpaslan, Y.B.; Eyduran, F.; Ozyurek, C.; Iskeleli, N.O. Experimental (C-13 NMR, H-1 NMR, FT-IR, single-crystal X-ray diffraction) and DFT studies on 3,4-bis(isopropylamino)cyclobut-3-ene-1,2-dione. *Spectrochim. Acta A* **2011**, *83*, 472–477. [[CrossRef](#)]
144. Silva, C.E.; Dos Santos, H.F.; Speziali, N.L.; Diniz, R.; de Oliveira, L.F.C. Role of the Substituent Effect over the Squarate Oxocarbonic Ring: Spectroscopy, Crystal Structure, and Density Functional Theory Calculations of 1,2-Dianilinosquairane. *J. Phys. Chem. A* **2010**, *114*, 10097–10109. [[CrossRef](#)]
145. Ximenis, M.; Bustelo, E.; Algarra, A.G.; Vega, M.; Rotger, C.; Basallote, M.G.; Costa, A. Kinetic Analysis and Mechanism of the Hydrolytic Degradation of Squaramides and Squaramic Acids. *J. Org. Chem.* **2017**, *82*, 2160–2170. [[CrossRef](#)]
146. Jiao, T.Y.; Wu, G.C.; Zhang, Y.; Shen, L.B.; Lei, Y.; Wang, C.Y.; Fahrenbach, A.C.; Li, H. Self-Assembly in Water with N-Substituted Imines. *Angew. Chem. Int. Ed.* **2020**, *59*, 18350–18367. [[CrossRef](#)]
147. Ortega-Castro, J.; Adrover, M.; Frau, J.; Salva, A.; Donoso, J.; Munoz, F. DFT studies on Schiff base formation of vitamin B6 analogues. Reaction between a pyridoxamine-analogue and carbonyl compounds. *J. Phys. Chem. A* **2010**, *114*, 4634–4640. [[CrossRef](#)]
148. Salva, A.; Donoso, J.; Frau, J.; Munoz, F. DFT studies on Schiff base formation of vitamin B-6 analogues. *J. Phys. Chem. A* **2003**, *107*, 9409–9414. [[CrossRef](#)]
149. Afonso, C.F.; Marques, M.C.; Antonio, J.P.M.; Cordeiro, C.; Gois, P.M.P.; Cal, P.; Bernardes, G.J.L. Cysteine-Assisted Click-Chemistry for Proximity-Driven, Site-Specific Acetylation of Histones. *Angew. Chem. Int. Ed. Engl.* **2022**, *61*, e202208543. [[CrossRef](#)] [[PubMed](#)]
150. Ahangarpour, M.; Kaviani, I.; Brimble, M.A. Thia-Michael addition: The route to promising opportunities for fast and cysteine-specific modification. *Org. Biomol. Chem.* **2023**, *21*, 3057–3072. [[CrossRef](#)] [[PubMed](#)]

151. Harel, O.; Jbara, M. Posttranslational Chemical Mutagenesis Methods to Insert Posttranslational Modifications into Recombinant Proteins. *Molecules* **2022**, *27*, 4389. [[CrossRef](#)] [[PubMed](#)]
152. Abdelsalam, A.M.; Somaida, A.; Ayoub, A.M.; Alsharif, F.M.; Preis, E.; Wojcik, M.; Bakowsky, U. Surface-Tailored Zein Nanoparticles: Strategies and Applications. *Pharmaceutics* **2021**, *13*, 1354. [[CrossRef](#)] [[PubMed](#)]
153. Stuparu, M.C.; Khan, A. Thiol-epoxy “click” chemistry: Application in preparation and postpolymerization modification of polymers. *J. Polym. Sci. Pol. Chem.* **2016**, *54*, 3057–3070. [[CrossRef](#)]
154. Liao, R.Z.; Thiel, W. Determinants of Regioselectivity and Chemoselectivity in Fosfomycin Resistance Protein FosA from QM/MM Calculations. *J. Phys. Chem. B* **2013**, *117*, 1326–1336. [[CrossRef](#)]
155. Senger, N.A.; Bo, B.; Cheng, Q.; Keeffe, J.R.; Gronert, S.; Wu, W.M. The Element Effect Revisited: Factors Determining Leaving Group Ability in Activated Nucleophilic Aromatic Substitution Reactions. *J. Org. Chem.* **2012**, *77*, 9535–9540. [[CrossRef](#)]
156. Northrop, B.H.; Frayne, S.H.; Choudhary, U. Thiol-maleimide “click” chemistry: Evaluating the influence of solvent, initiator, and thiol on the reaction mechanism, kinetics, and selectivity. *Polym. Chem.* **2015**, *6*, 3415–3430. [[CrossRef](#)]
157. Raycroft, M.A.R.; Racine, K.E.; Rowley, C.N.; Keillor, J.W. Mechanisms of Alkyl and Aryl Thiol Addition to N-Methylmaleimide. *J. Org. Chem.* **2018**, *83*, 11674–11685. [[CrossRef](#)]
158. Moran, D.; Sukcharoenphon, K.; Puchta, R.; Schaefer, H.F.; Schleyer, P.V.; Hoff, C.D. 2-pyridinethiol/2-pyridinethione tautomeric equilibrium. A comparative experimental and computational study. *J. Org. Chem.* **2002**, *67*, 9061–9069. [[CrossRef](#)]
159. Dahl, K.H.; McKinley-McKee, J.S. The reactivity of affinity labels: A kinetic study of the reaction of alkyl halides with thiolate anions—A model reaction for protein alkylation. *Bioorg. Chem.* **1981**, *10*, 329–341. [[CrossRef](#)]
160. Wang, H.; Vath, G.M.; Gleason, K.J.; Hanna, P.E.; Wagner, C.R. Probing the mechanism of hamster arylamine N-acetyltransferase 2 acetylation by active site modification, site-directed mutagenesis, and pre-steady state and steady state kinetic studies. *Biochemistry* **2004**, *43*, 8234–8246. [[CrossRef](#)]
161. Pals, J.A.; Wagner, E.D.; Plewa, M.J. Energy of the Lowest Unoccupied Molecular Orbital, Thiol Reactivity, and Toxicity of Three Monobrominated Water Disinfection Byproducts. *Environ. Sci. Technol.* **2016**, *50*, 3215–3221. [[CrossRef](#)]
162. Desai, K.K.; Miller, B.G. Recruitment of genes and enzymes conferring resistance to the nonnatural toxin bromoacetate. *Proc. Natl. Acad. Sci. USA* **2010**, *107*, 17968–17973. [[CrossRef](#)] [[PubMed](#)]
163. Ferreira, V.F.C.; Oliveira, B.L.; D’Onofrio, A.; Farinha, C.M.; Gano, L.; Paulo, A.; Bernardes, G.J.L.; Mendes, F. In Vivo Pretargeting Based on Cysteine-Selective Antibody Modification with IEDDA Bioorthogonal Handles for Click Chemistry. *Bioconjug. Chem.* **2021**, *32*, 121–132. [[CrossRef](#)] [[PubMed](#)]
164. Ochtrop, P.; Hackenberger, C.P.R. Recent advances of thiol-selective bioconjugation reactions. *Curr. Opin. Chem. Biol.* **2020**, *58*, 28–36. [[CrossRef](#)]
165. Beck, A.; Goetsch, L.; Dumontet, C.; Corvaia, N. Strategies and challenges for the next generation of antibody-drug conjugates. *Nat. Rev. Drug Discov.* **2017**, *16*, 315–337. [[CrossRef](#)]
166. Smith, M.E.; Schumacher, F.F.; Ryan, C.P.; Tedaldi, L.M.; Papaioannou, D.; Waksman, G.; Caddick, S.; Baker, J.R. Protein modification, bioconjugation, and disulfide bridging using bromomaleimides. *J. Am. Chem. Soc.* **2010**, *132*, 1960–1965. [[CrossRef](#)]
167. Feuillatre, O.; Gely, C.; Huvelle, S.; Baltus, C.B.; Juen, L.; Joubert, N.; Desgranges, A.; Viaud-Massuard, M.C.; Martin, C. Impact of Maleimide Disubstitution on Chemical and Biological Characteristics of HER2 Antibody-Drug Conjugates. *ACS Omega* **2020**, *5*, 1557–1565. [[CrossRef](#)]
168. Tedaldi, L.M.; Smith, M.E.; Nathani, R.I.; Baker, J.R. Bromomaleimides: New reagents for the selective and reversible modification of cysteine. *Chem. Commun.* **2009**, *45*, 6583–6585. [[CrossRef](#)]
169. Karabacak, M.; Coruh, A.; Kurt, M. FT-IR, FT-Raman, NMR spectra, and molecular structure investigation of 2,3-dibromo-N-methylmaleimide: A combined experimental and theoretical study. *J. Mol. Struct.* **2008**, *892*, 125–131. [[CrossRef](#)]
170. Scinto, S.L.; Bilodeau, D.A.; Hincapie, R.; Lee, W.; Nguyen, S.S.; Xu, M.; Am Ende, C.W.; Finn, M.G.; Lang, K.; Lin, Q.; et al. Bioorthogonal chemistry. *Nat. Rev. Methods Primers* **2021**, *1*, 30. [[CrossRef](#)] [[PubMed](#)]
171. Aarjane, M.; Slassi, S.; Amine, A. Novel series of N-acylhydrazone based on acridone: Synthesis, conformational and theoretical studies. *J. Mol. Struct.* **2021**, *1225*, 129079. [[CrossRef](#)]
172. Kolb, H.C.; Finn, M.G.; Sharpless, K.B. Click Chemistry: Diverse Chemical Function from a Few Good Reactions. *Angew. Chem. Int. Ed. Engl.* **2001**, *40*, 2004–2021. [[CrossRef](#)] [[PubMed](#)]
173. Devaraj, N.K.; Finn, M.G. Introduction: Click Chemistry. *Chem. Rev.* **2021**, *121*, 6697–6698. [[CrossRef](#)]
174. Adumeau, P.; Sharma, S.K.; Brent, C.; Zeglis, B.M. Site-Specifically Labeled Immunoconjugates for Molecular Imaging—Part 2: Peptide Tags and Unnatural Amino Acids. *Mol. Imaging Biol.* **2016**, *18*, 153–165. [[CrossRef](#)]
175. Kim, C.H.; Axup, J.Y.; Schultz, P.G. Protein conjugation with genetically encoded unnatural amino acids. *Curr. Opin. Chem. Biol.* **2013**, *17*, 412–419. [[CrossRef](#)]
176. Sarrett, S.M.; Keinanen, O.; Dayts, E.J.; Dewaele-Le Roi, G.; Rodriguez, C.; Carnazza, K.E.; Zeglis, B.M. Inverse electron demand Diels-Alder click chemistry for pretargeted PET imaging and radioimmunotherapy. *Nat. Protoc.* **2021**, *16*, 3348–3381. [[CrossRef](#)]
177. Beck, S.; Schultze, J.; Rader, H.J.; Holm, R.; Schinnerer, M.; Barz, M.; Koynov, K.; Zentel, R. Site-Specific DBCO Modification of DEC205 Antibody for Polymer Conjugation. *Polymers* **2018**, *10*, 141. [[CrossRef](#)]
178. Spampinato, A.; Kuzmova, E.; Pohl, R.; Sykorova, V.; Vrabel, M.; Kraus, T.; Hocek, M. trans-Cyclooctene- and Bicyclononyne-Linked Nucleotides for Click Modification of DNA with Fluorogenic Tetrazines and Live Cell Metabolic Labeling and Imaging. *Bioconjug. Chem.* **2023**, *34*, 772–780. [[CrossRef](#)]

179. Wagner, J.A.; Mercadante, D.; Nikić, I.; Lemke, E.A.; Grater, F. Origin of Orthogonality of Strain-Promoted Click Reactions. *Chemistry* **2015**, *21*, 12431–12435. [[CrossRef](#)] [[PubMed](#)]
180. Garcia-Aznar, P.; Escorihuela, J. Computational insights into the inverse electron-demand Diels-Alder reaction of norbornenes with 1,2,4,5-tetrazines: Norbornene substituents' effects on the reaction rate. *Org. Biomol. Chem.* **2022**, *20*, 6400–6412. [[CrossRef](#)]
181. Battisti, U.M.; Garcia-Vazquez, R.; Svatunek, D.; Herrmann, B.; Löffler, A.; Mikula, H.; Herth, M.M. Synergistic Experimental and Computational Investigation of the Bioorthogonal Reactivity of Substituted Aryltetrazines. *Bioconjug. Chem.* **2022**, *33*, 608–624. [[CrossRef](#)] [[PubMed](#)]
182. Svatunek, D.; Denk, C.; Mikula, H. A computational model to predict the Diels-Alder reactivity of aryl/alkyl-substituted tetrazines. *Monatsh. Chem.* **2018**, *149*, 833–837. [[CrossRef](#)] [[PubMed](#)]
183. Xie, S.; Sundhoro, M.; Houk, K.N.; Yan, M. Electrophilic Azides for Materials Synthesis and Chemical Biology. *Acc. Chem. Res.* **2020**, *53*, 937–948. [[CrossRef](#)]
184. Baldensperger, T.; Glomb, M.A. Pathways of Non-enzymatic Lysine Acylation. *Front. Cell Dev. Biol.* **2021**, *9*, 664553. [[CrossRef](#)]
185. Lammers, M. Post-translational Lysine Ac(ety)lation in Bacteria: A Biochemical, Structural, and Synthetic Biological Perspective. *Front. Microbiol.* **2021**, *12*, 757179. [[CrossRef](#)]
186. Wang, M.M.; You, D.; Ye, B.C. Site-specific and kinetic characterization of enzymatic and nonenzymatic protein acetylation in bacteria. *Sci. Rep.* **2017**, *7*, 14790. [[CrossRef](#)]
187. Simić, Z.; Weiwad, M.; Schierhorn, A.; Steegborn, C.; Schutkowski, M. The epsilon-Amino Group of Protein Lysine Residues Is Highly Susceptible to Nonenzymatic Acylation by Several Physiological Acyl-CoA Thioesters. *Chembiochem* **2015**, *16*, 2337–2347. [[CrossRef](#)]
188. Carrico, C.; Cruz, A.; Walter, M.; Meyer, J.; Wehrfritz, C.; Shah, S.; Wei, L.; Schilling, B.; Verdin, E. Coenzyme A binding sites induce proximal acylation across protein families. *Sci. Rep.* **2023**, *13*, 5029. [[CrossRef](#)]
189. Faulkner, S.; Maksimovic, I.; David, Y. A chemical field guide to histone nonenzymatic modifications. *Curr. Opin. Chem. Biol.* **2021**, *63*, 180–187. [[CrossRef](#)] [[PubMed](#)]
190. Graf, L.G.; Vogt, R.; Blasl, A.T.; Qin, C.; Schulze, S.; Zuhlke, D.; Sievers, S.; Lammers, M. Assays to Study Enzymatic and Non-Enzymatic Protein Lysine Acetylation In Vitro. *Curr. Protoc.* **2021**, *1*, e277. [[CrossRef](#)]
191. Maksimovic, I.; David, Y. Non-enzymatic Covalent Modifications as a New Chapter in the Histone Code. *Trends Biochem. Sci.* **2021**, *46*, 718–730. [[CrossRef](#)]
192. Baeza, J.; Smallegan, M.J.; Denu, J.M. Site-specific reactivity of nonenzymatic lysine acetylation. *ACS Chem. Biol.* **2015**, *10*, 122–128. [[CrossRef](#)] [[PubMed](#)]
193. Giangregorio, N.; Tonazzi, A.; Console, L.; Indiveri, C. Post-translational modification by acetylation regulates the mitochondrial carnitine/acylcarnitine transport protein. *Mol. Cell. Biochem.* **2017**, *426*, 65–73. [[CrossRef](#)]
194. Hong, S.Y.; Ng, L.T.; Ng, L.F.; Inoue, T.; Tolwinski, N.S.; Hagen, T.; Gruber, J. The Role of Mitochondrial Non-Enzymatic Protein Acylation in Ageing. *PLoS ONE* **2016**, *11*, e0168752. [[CrossRef](#)]
195. Kerner, J.; Yohannes, E.; Lee, K.; Virmani, A.; Koverech, A.; Cavazza, C.; Chance, M.R.; Hoppel, C. Acetyl-L-carnitine increases mitochondrial protein acetylation in the aged rat heart. *Mech. Ageing Dev.* **2015**, *145*, 39–50. [[CrossRef](#)]
196. Martin, W.F.; Thauer, R.K. Energy in Ancient Metabolism. *Cell* **2017**, *168*, 953–955. [[CrossRef](#)] [[PubMed](#)]
197. Semenov, S.N.; Kraft, L.J.; Ainla, A.; Zhao, M.; Baghbanzadeh, M.; Campbell, V.E.; Kang, K.; Fox, J.M.; Whitesides, G.M. Autocatalytic, bistable, oscillatory networks of biologically relevant organic reactions. *Nature* **2016**, *537*, 656–660. [[CrossRef](#)] [[PubMed](#)]
198. Shalayel, I.; Leqraa, N.; Blandin, V.; Vallée, Y. Catalysis before Enzymes: Thiol-Rich Peptides as Molecular Diversity Providers on the Early Earth. *Diversity* **2023**, *15*, 256. [[CrossRef](#)]
199. Chevallot-Beroux, E.; Gorges, J.; Moran, J. Energy Conservation via Thioesters in a Non-enzymatic Metabolism-like Reaction Network. *ChemRxiv* **2019**, 1–10. [[CrossRef](#)]
200. De Duve, C. A research proposal on the origin of life. *Orig. Life Evol. Biosph.* **2003**, *33*, 559–574. [[CrossRef](#)] [[PubMed](#)]
201. Harmel, R.; Fiedler, D. Features and regulation of non-enzymatic post-translational modifications. *Nat. Chem. Biol.* **2018**, *14*, 244–252. [[CrossRef](#)] [[PubMed](#)]
202. Sousa Silva, M.; Gomes, R.A.; Ferreira, A.E.; Ponces Freire, A.; Cordeiro, C. The glyoxalase pathway: The first hundred years... and beyond. *Biochem. J.* **2013**, *453*, 1–15. [[CrossRef](#)]
203. Honek, J.F. Glyoxalase biochemistry. *Biomol. Concepts* **2015**, *6*, 401–414. [[CrossRef](#)] [[PubMed](#)]
204. Varner, E.L.; Trefely, S.; Bartee, D.; von Krusenstiern, E.; Izzo, L.; Bekeova, C.; O'Connor, R.S.; Seifert, E.L.; Wellen, K.E.; Meier, J.L.; et al. Quantification of lactoyl-CoA (lactyl-CoA) by liquid chromatography mass spectrometry in mammalian cells and tissues. *Open Biol.* **2020**, *10*, 200187. [[CrossRef](#)]
205. Wolfenden, R.; Liang, Y.L. Contributions of Solvent Water to Biological Group-Transfer Potentials: Mixed Anhydrides of Phosphoric and Carboxylic Acids. *Bioorg. Chem.* **1989**, *17*, 486–489. [[CrossRef](#)]
206. Weinert, B.T.; Iesmantavicius, V.; Wagner, S.A.; Scholz, C.; Gummesson, B.; Beli, P.; Nystrom, T.; Choudhary, C. Acetyl-phosphate is a critical determinant of lysine acetylation in *E. coli*. *Mol. Cell* **2013**, *51*, 265–272. [[CrossRef](#)]
207. Kluger, R.; Tsui, W.C. Methyl Acetyl Phosphate—A Small Anionic Acetylating Agent. *J. Org. Chem.* **1980**, *45*, 2723–2724. [[CrossRef](#)]

208. Ueno, H.; Pospischil, M.A.; Kluger, R.; Manning, J.M. Methyl Acetyl Phosphate—A Novel Acetylating Agent Its Site-Specific Modification of Human Hemoglobin-A. *J. Chromatogr.* **1986**, *359*, 193–201. [[CrossRef](#)]
209. Ueno, H.; Pospischil, M.A.; Manning, J.M.; Kluger, R. Site-Specific Modification of Hemoglobin by Methyl Acetyl Phosphate. *Arch. Biochem. Biophys.* **1986**, *244*, 795–800. [[CrossRef](#)] [[PubMed](#)]
210. Kluger, R. 1994 Syntex Award Lecture—Anionic Electrophiles, Protein Modification, and Artificial Blood. *Can. J. Chem.* **1994**, *72*, 2193–2197. [[CrossRef](#)]
211. Kataoka, K.; Tanizawa, K.; Fukui, T.; Ueno, H.; Yoshimura, T.; Esaki, N.; Soda, K. Identification of active site lysyl residues of phenylalanine dehydrogenase by chemical modification with methyl acetyl phosphate combined with site-directed mutagenesis. *J. Biochem.* **1994**, *116*, 1370–1376. [[CrossRef](#)] [[PubMed](#)]
212. Fritz, I.B.; Schultz, S.K.; Srere, P.A. Properties of partially purified carnitine acetyltransferase. *J. Biol. Chem.* **1963**, *238*, 2509–2517. [[CrossRef](#)]
213. Muller, D.M.; Strack, E. The binding energy of the ester group in O-acylcarnitines and some carboxyl derivatives, III. Hydrolysis enthalpy of O-acylcarnitines and betaine esters (author's transl). *Hoppe Seylers Z. Physiol. Chem.* **1973**, *354*, 1091–1096. [[CrossRef](#)] [[PubMed](#)]
214. Pieklik, J.R.; Guynn, R.W. Equilibrium constants of the reactions of choline acetyltransferase, carnitine acetyltransferase, and acetylcholinesterase under physiological conditions. *J. Biol. Chem.* **1975**, *250*, 4445–4450. [[CrossRef](#)]
215. Colucci, W.J.; Gandour, R.D. Carnitine Acetyltransferase—A Review of Its Biology, Enzymology, and Bioorganic Chemistry. *Bioorg. Chem.* **1988**, *16*, 307–334. [[CrossRef](#)]
216. Gandour, R.D. Rationalizing the solution properties of zwitterions by means of computational chemistry. *Chem. Biodivers.* **2005**, *2*, 1580–1594. [[CrossRef](#)]
217. Dewar, M.J.S.; Zebisch, E.G.; Healy, E.F.; Stewart, J.J.P. Development and use of quantum mechanical molecular models. 76. AM1: A new general purpose quantum mechanical molecular model. *J. Am. Chem. Soc.* **1985**, *107*, 3902–3909. [[CrossRef](#)]
218. Klamt, A.; Moya, C.; Palomar, J. A comprehensive comparison of the IEFPCM and SS(V)PE continuum solvation methods with the COSMO approach. *J. Chem. Theory. Comput.* **2015**, *11*, 4220–4225. [[CrossRef](#)]
219. Rosas-Garcia, V.M.; Gandour, R.D. Conformationally-Dependent Free Energies of Solvation. An Explanation for the Large Group-Transfer Potential of Acetylcarnitine. *J. Am. Chem. Soc.* **1997**, *119*, 7587–7588. [[CrossRef](#)]
220. Ferri, L.; Jocelyn, P.C.; Siliprandi, N. The mitochondrial handling of D,L-thiocarnitine and its S-acetyl derivative. *FEBS Lett.* **1980**, *121*, 19–22. [[CrossRef](#)] [[PubMed](#)]
221. Stern, J.R.; Drummond, G.I. Enzymes of ketone body metabolism. III. Enzymic thiolysis of acetoacetyl coenzyme A and acetoacetyl-pantetheine by mono- and dithiol compounds. *J. Biol. Chem.* **1961**, *236*, 2892–2897. [[CrossRef](#)] [[PubMed](#)]
222. Smith, M.B. *March's Advanced Organic Chemistry: Reactions, Mechanisms, and Structure*, 7th ed.; John Wiley & Sons, Inc.: Hoboken, NJ, USA, 2013.
223. Vane, J.R. Inhibition of prostaglandin synthesis as a mechanism of action for aspirin-like drugs. *Nat. New Biol.* **1971**, *231*, 232–235. [[CrossRef](#)] [[PubMed](#)]
224. Vane, J.R.; Botting, R.M. The mechanism of action of aspirin. *Thromb. Res.* **2003**, *110*, 255–258. [[CrossRef](#)]
225. Thomas, G. *Medicinal Chemistry*, 2nd ed.; John Wiley & Sons, Ltd.: Chichester, UK, 2007.
226. Palmer, M.; Chan, A.; Dieckmann, T.; Honek, J. *Biochemical Pharmacology*; John Wiley & Sons, Ltd.: Hoboken, NJ, USA, 2012.
227. Alfonso, L.F.; Srivenugopal, K.S.; Bhat, G.J. Does aspirin acetylate multiple cellular proteins? (Review). *Mol. Med. Rep.* **2009**, *2*, 533–537. [[CrossRef](#)]
228. Wang, J.; Zhang, C.J.; Zhang, J.; He, Y.; Lee, Y.M.; Chen, S.; Lim, T.K.; Ng, S.; Shen, H.M.; Lin, Q. Mapping sites of aspirin-induced acetylations in live cells by quantitative acid-cleavable activity-based protein profiling (QA-ABPP). *Sci. Rep.* **2015**, *5*, 7896. [[CrossRef](#)] [[PubMed](#)]
229. Bateman, L.A.; Zaro, B.W.; Miller, S.M.; Pratt, M.R. An alkyne-aspirin chemical reporter for the detection of aspirin-dependent protein modification in living cells. *J. Am. Chem. Soc.* **2013**, *135*, 14568–14573. [[CrossRef](#)]
230. Mikkelsen, S.R.; Cortón, E. *Bioanalytical Chemistry*; John Wiley & Sons, Ltd.: Hoboken, NJ, USA, 2004.
231. Bisswanger, H. *Practical Enzymology*, 2nd ed.; Wiley-Blackwell: Weinheim, Germany, 2011.
232. Breidenbach, J.; Bartz, U.; Gutschow, M. Coumarin as a structural component of substrates and probes for serine and cysteine proteases. *Biochim. Biophys. Acta Proteins Proteom.* **2020**, *1868*, 140445. [[CrossRef](#)]
233. Means, G.E.; Bender, M.L. Acetylation of human serum albumin by p-nitrophenyl acetate. *Biochemistry* **1975**, *14*, 4989–4994. [[CrossRef](#)]
234. Bhatt, A.N.; Rai, Y.; Verma, A.; Pandey, S.; Kaushik, K.; Parmar, V.S.; Arya, A.; Prasad, A.K.; Dwarakanath, B.S. Non-Enzymatic Protein Acetylation by 7-Acetoxy-4-Methylcoumarin: Implications in Protein Biochemistry. *Protein Pept. Lett.* **2020**, *27*, 736–743. [[CrossRef](#)]
235. Raj, H.G.; Parmar, V.S.; Jain, S.C.; Goel, S.; Singh, A.; Tyagi, Y.K.; Jha, H.N.; Olsen, C.E.; Wengel, J. Mechanism of biochemical action of substituted 4-methylbenzopyran-2-ones. Part 4: Hyperbolic activation of rat liver microsomal NADPH cytochrome C reductase by the novel acetylator 7,8-diacetoxy-4-methylcoumarin. *Bioorg. Med. Chem.* **1999**, *7*, 369–373. [[CrossRef](#)] [[PubMed](#)]

236. Raj, H.G.; Parmar, V.S.; Jain, S.C.; Kohli, E.; Ahmad, N.; Goel, S.; Tyagi, Y.K.; Sharma, S.K.; Wengel, J.; Olsen, C.E. Mechanism of biochemical action of substituted 4-methylbenzopyran-2-ones. Part 7: Assay and characterization of 7,8-diacetoxy-4-methylcoumarin: Protein transacetylase from rat liver microsomes based on the irreversible inhibition of cytosolic glutathione S-transferase. *Bioorg. Med. Chem.* **2000**, *8*, 1707–1712. [[CrossRef](#)]
237. Pillaiyar, T.; Flury, P.; Kruger, N.; Su, H.; Schakel, L.; Barbosa Da Silva, E.; Eppler, O.; Kronenberger, T.; Nie, T.; Luedtke, S.; et al. Small-Molecule Thioesters as SARS-CoV-2 Main Protease Inhibitors: Enzyme Inhibition, Structure-Activity Relationships, Antiviral Activity, and X-ray Structure Determination. *J. Med. Chem.* **2022**, *65*, 9376–9395. [[CrossRef](#)] [[PubMed](#)]

**Disclaimer/Publisher's Note:** The statements, opinions and data contained in all publications are solely those of the individual author(s) and contributor(s) and not of MDPI and/or the editor(s). MDPI and/or the editor(s) disclaim responsibility for any injury to people or property resulting from any ideas, methods, instructions or products referred to in the content.